



**Politecnico  
di Torino**

Politecnico di Torino

Master's Degree Thesis

**The runoff coefficient for a T-year  
design flood, using data from  
Austrian catchments**

Master's degree course in Environmental and Land Engineering

**Thesis Advisor:**

Alberto Viglione  
Günter Blöschl

**Candidate:**

Lorenzo Ceretti  
matricola 290226

March, 2023



*Dream until it's your reality*



## Abstract

The runoff coefficient is the percentage of rainfall that becomes runoff (and river discharge) during a storm, and it has a relevant role in engineering practice. It is, in fact, a key parameter in the so called "design-storm" method, in which hypothetical storm events of a given return period are transformed into flood discharges that are assumed to have the same return period. In order to investigate what values of runoff coefficient should be used in the design-storm method, in this study we analyse the correlation between event runoff coefficients and catchment characteristics, accounting for the relationship between the return periods of the storms and of the flood peaks. We estimate the runoff coefficient for flood events from hourly rainfall and runoff timeseries for several catchments in eastern Austria. Each event is identified with an automatic procedure based on three main steps: (1) baseflow separation from direct runoff in the discharge timeseries; (2) identification of every single event starting from the largest peak flow to the smallest ones exceeding a pre-defined threshold; (3) estimation of the event runoff coefficient using a rainfall-runoff model that minimizes the root mean square between the observed and the modelled runoff. For each event, we then estimate the return period associated with the respective peak flow ( $T_Q$ ) and maximum precipitation for different durations ( $T_P$ ). Results indicate that  $T_Q$  can be much higher than the corresponding  $T_P$  and that their relationship is related mainly to the wetness of the system, represented by the event runoff coefficient. It is also recognisable a dependency of the runoff coefficient with the return periods of rainfall and runoff, since the runoff coefficient increases moving towards extreme peak discharge values. In engineering practice, the median value of the distribution of runoff coefficients is usually adopted, in order to transform the design-storm into a flood peak with the same return period, but this may not be the right choice. Our results show that, because of the dependency of the runoff coefficient on the return periods and the high variability found in real events, it is difficult to choose the proper value in a simple way. We find that the value of the runoff coefficients for which  $T_Q$  is close to  $T_P$  in real events varies very much for small events but, for large events with return periods of the order of 10 years or more, tends to stabilise around the value that is exceeded 80% of the times, considering the distribution of runoff coefficients for all events. In the region of interest, i.e., eastern Austria, these runoff coefficients have values close to 0.4.



# Contents

List of Figures	v
List of Tables	ix
<b>1 Introduction</b>	<b>1</b>
<b>2 State of the art</b>	<b>3</b>
2.1 Austrian hydrological conditions . . . . .	3
2.2 Role of the soil moisture . . . . .	6
2.3 Duration of rainfall and flood events . . . . .	7
2.3.1 Rainfall duration . . . . .	7
2.3.2 Flood duration . . . . .	8
2.3.3 Critical storm duration . . . . .	9
2.4 Runoff coefficient distribution through Monte-Carlo simulation . . .	10
<b>3 Data</b>	<b>13</b>
3.1 Starting data set . . . . .	13
3.1.1 Rainfall interpolation . . . . .	13
3.1.2 Runoff data . . . . .	14
3.2 Area of study . . . . .	15
<b>4 Methodology</b>	<b>19</b>
4.1 Introduction . . . . .	19
4.2 Statistical analysis . . . . .	19
4.2.1 General terminology . . . . .	20
4.2.2 Frequency analysis . . . . .	20
4.3 Events data . . . . .	21
4.3.1 Base flow separation . . . . .	22
4.3.2 Event separation . . . . .	22
4.3.3 Attribution of rainfall events . . . . .	23
4.4 Catchment and event characteristics . . . . .	24
4.4.1 Event characteristics . . . . .	24

4.5	Definition of storm return period . . . . .	25
4.5.1	Extraction of the annual maximum rainfall intensity . . . . .	25
4.5.2	Frequency analysis of the annual rainfall data . . . . .	25
4.5.3	Frequency analysis of the event runoff intensity . . . . .	27
4.6	Seasons . . . . .	28
4.7	Spearman correlation . . . . .	28
<b>5</b>	<b>Results</b>	<b>31</b>
5.1	Events extracted . . . . .	31
5.2	Plotting position and IDF curve . . . . .	32
5.3	Runoff return period . . . . .	34
5.4	Runoff regime . . . . .	34
5.5	Runoff coefficients distribution . . . . .	38
5.6	Ratio between return periods . . . . .	40
5.7	Probability distribution of runoff coefficients . . . . .	43
5.8	Season analysis . . . . .	46
<b>6</b>	<b>Discussions and conclusions</b>	<b>49</b>
<b>A</b>	<b>Appendix 1</b>	<b>A1</b>
A.1	Generalized Pareto code . . . . .	A1
A.2	Event separation code . . . . .	A2
<b>B</b>	<b>Figures out of text</b>	<b>B1</b>
B.1	Starting data set . . . . .	B2
B.2	IDF curves . . . . .	B7
B.3	QDF curves . . . . .	B11
B.4	Comparison between return periods . . . . .	B14
B.5	Ratio between return periods . . . . .	B17
B.6	HydroCarpath conference . . . . .	B22

**References**

# List of Figures

2.1	Location of hydrological regions in Austria. Numbers have been plotted at the location of each stream gauge, (Merz & Blöschl, 2009)	3
2.2	Location of regions with similar distribution functions of event runoff coefficients. Numbers have been plotted at the location of each gauged catchment and refer to the group (Merz, Blöschl, & Parajka, 2006).	5
2.3	Event runoff depth vs. event rainfall (including snowmelt) for four catchments in Austria. (a) Ritzenried/Pitze (220 km <sup>2</sup> ); (b) Lunz am See/Ois (117 km <sup>2</sup> ); (c) Zwettl/Kamp, (622 km <sup>2</sup> ); (d) Schützen am Gebirge/Wulka (384 km <sup>2</sup> ).	5
2.4	Spatial pattern of the scaling parameter $\eta_p$ used in Breinl, Lun, Müller-Thomy, and Blöschl (2021) as one of the rainfall model parameters studied. Colored points represent the rain gauges inside the different hydroclimatic regions.	7
2.5	Distribution function of event runoff coefficient deviates stratified by (left) small (dashed lines) and large (solid lines) event rainfall depth, (middle) lower (dashed lines) and high (solid lines) maximum event rainfall intensity, and (right) shorter (dashed lines) and longer (solid lines) rainfall duration (Merz & Blöschl, 2009).	8
2.6	Median of flood timescale for each catchment as a function of catchment area. Each line represent a studied hot spot in Gaál et al. (2012).	8
2.7	Median of flood timescale in Austria plotted versus catchment area (km <sup>2</sup> , (Gaál et al., 2012).	9
2.8	Mapping of return periods obtained simulating 100 000 years of events. Events characterized by high runoff coefficients are dark-blue while low runoff coefficient events are represented in light-green (Viglione, Merz, & Blöschl, 2009b).	10

2.9	Relationship between rainfall return periods $T_P$ and flood return periods $T_Q$ for beta distributed runoff coefficients $r_c$ independent from the rainfall events. The three upper Panels (a), (c) and (e) represent the mapping of $T_P$ vs. $T_Q$ . The crosses are obtained by Monte- Carlo simulations (100 000 years). The envelope curves (continuous lines) are calculated analytically. The three lower Panels (b), (d) and (f) represent one horizontal slice ( $T_Q = 100$ years) of Panels (a), (c) and (e) respectively in terms of the ratio of return periods $T_Q/T_P$ . The parameters of the beta distribution are: Panels (a) and (b) – Dry system with average runoff coefficient $\delta_c = 0.1$ and variance $\sigma_c^2 = 0.009$ ( $CV_c = 0.95$ ); Panels (c) and (d) – Wetter system with $\delta_c = 0.3$ and $\sigma_c^2 = 0.038$ ( $CV_c = 0.65$ ); Panels (e) and (f) – Very wet system with $\delta_c = 0.7$ and $\sigma_c^2 = 0.022$ ( $CV_c = 0.21$ ) (Viglione et al., 2009b).	11
2.10	Runoff coefficients $r_{1:1}$ that give a 1 to 1 correspondence between rainfall and flood return periods plotted against return period. Panel (a) – Runoff coefficient $r_{1:1}$ ; Panel (b) – Non-exceedance frequency of $r_{1:1}$ on the parent distributions of $r_c$ . The parent beta distributions correspond to the seven wetness conditions labeled with seven different runoff coefficients (from dry to wet systems) (Viglione et al., 2009b).	12
3.1	Available data set for the entire Austria with Stream gauge and Rainfall gauge location.	14
3.2	Location of the stream gauges considered in the thesis. Only catchments with an area between 80 and 600 km <sup>2</sup> are considered.	15
3.3	Total duration series for a single catchment. The black line represents runoff data while the blue bars represent rainfall series	17
4.1	Example of hydrologic data arranged according to the time of occurrence (Chow, 1964).	21
4.2	Hydrograph and hyetograph for an identified event with Chapman and Maxwell filter. The dotted line represents the baseflow, the solid line represents the observed runoff and the blue bars represent the event rainfall.	23

4.3	Example of IDF curve for each time window within each single event.	26
4.4	Example of IDF curve for each time window within each single event. Generalized Pareto distribution has been fitted to each single set of data. . . . .	27
4.5	Description of a box plot with its quartiles. The Lower Quartile represents the 25th percentile of the distribution and the Upper Quartile represents the 75th percentile of the distribution. . . . .	29
5.1	Number of events extracted for each single catchment. . . . .	31
5.2	Example of three hydropragh and hyetograph extracted, representing three months in which some events are depicted . . . . .	33
5.3	Event runoff depth vs. event rainfall volume for all the catchments analysed. The plots are divided in two separated figures. The other six catchments are in Fig. 5.4. . . . .	36
5.4	Event runoff depth vs. event rainfall volume for all the catchments analysed. The plots are divided in two separated figures. The other six catchments are in Fig. 5.3. . . . .	37
5.5	Average runoff coefficient of each single catchment as a function of the variability of the events. . . . .	38
5.6	Relationship between rainfall return period $T_P$ and runoff return period $T_Q$ for every catchment analysed. Each single point correspond to a single event and it is coloured according to its runoff coefficient. Here the rainfall return period is the one with the duration that produce the higher return period. . . . .	39
5.7	Relationship between the ratio of return periods $T_Q/T_P$ and the runoff coefficient for each catchment analysed. Each point represent a single event; the ratio between the return periods has been calculated with the maximum rainfall return period among all the "duration" in the IDF curve. . . . .	42
5.8	Relationship between the ratio of return periods $T_Q/T_P$ and the runoff coefficient for each catchment analysed. This figure represent a slice of the Fig. 5.7 to better understand the behaviour of the events in a region in which the engineering practice is interested. . .	43

*List of Figures*

---

5.9	Relationship between the runoff coefficient of every event,with a ratio $T_Q = T_P$ in a range from 0.5 to 1.5, and the return period. . . . .	44
5.10	Probability of non-exceedance of runoff coefficient in two different situation. The first one take into consideration every events that have been extracted while the second one considers only those event in the range of $T_Q/T_P$ from 0.5 to 1.5 . . . . .	45
5.11	Probability of non-exceedance of the event runoff coefficients $r_{1:1}$ as a function of the return period. In this plot are reported the events in which $T_Q=T_P$ of every catchment. . . . .	46
5.12	Box plots of event runoff coefficient distribution according to the season. In this graph all the events extraced are considered and divided by season based on the first day of the event. . . . .	47
5.13	Box plots of event runoff coefficient distribution according to the season. In this graph only the events with a ratio $T_Q/T_P$ in a range between 0.5 and 1.5 are considered. . . . .	48

# List of Tables

3.1	Information of the catchments involved in the study. This table describes the characteristics of the stream station reported in Fig. 3.2. The MAPs are calculated from the stream data available. . . .	16
5.1	Different value of runoff coefficient based on the season analysis. . .	47
B.1	Information of the catchments involved in the study . . . . .	B1



# Introduction

The runoff coefficient considers the amount of rainfall that becomes direct runoff. It is back calculated from the volume of rainfall fallen in the watershed considered and from the volume of direct runoff measured in a river station during an event.

Understanding the physical processes that generate floods for a given period of occurrence is one of the most fascinating issue about catchments hydrology. These processes are not only complex because they are controlled by a large variability of variables such as rainfall, snowfall and catchment characteristics, but also because the interaction between each other plays a role in the phenomena and it is difficult to describe and to analyse.

Hydrological system can be well interpreted, and also in a simple way, by the statistical distribution, but it does not provide any knowledge on the physics beyond the flood processes. Moreover, from a predictive point of view, statistical analysis works in a pretty good manner only within the sample characteristics and assumption but, it is poorly relatable if any condition changes.

The statistical approach is the only method to retrieve information about flood and hydrology in general, but there are some issues that cannot be explained in a simple way. One of these is the common assumption, in the design storm procedure, that the return period of rainfall needs to be equal to the return period of the flood associated. Several studies demonstrate that, because of different processes occurring in the environment, the extreme storm usually does not produce an extreme flood; on the other hand an extreme flood could be produced by an extreme storm. The second case is rarer than the first one but it is still possible. As shown in chapter 5.6 there can be a lot of situations in which the return periods of rainfall and flood are different and the causes are difficult to be associated.

There are several studies in which processes causing floods are observed and studied in small catchments through a detailed instrumentation. However, at re-

gional scale such as Austria or even a part of Austria, it is far more difficult to detect these processes and to correlate them to flood.

The aim of this study is to analyse the correlation between the event runoff coefficient and catchment characteristics, with respect to the return period of the storm and of the flood peak. The final goal is to detect a value of the runoff coefficient that gives the discharge return period equal to the rainfall return period, which is typically assumed in the design storm procedure.

This may allow a better understanding in processes that cause floods, in which characteristics affect the generation of floods and a possible generalization of the assumption for which the return periods are equal.

## State of the art

### 2.1 Austrian hydrological conditions

Because of the large diversity of the hydrological conditions, austrian territory, and so austrian catchments, have been classified in five different hydroclimatic regions.

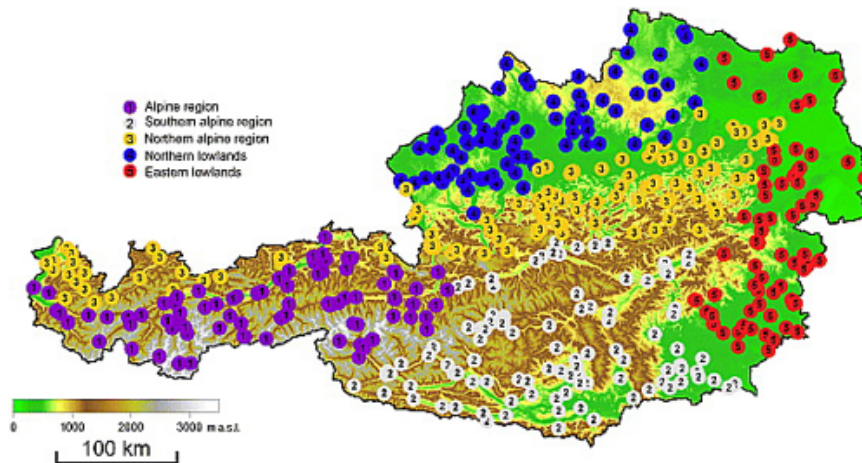


**Fig. 2.1.** Location of hydrological regions in Austria. Numbers have been plotted at the location of each stream gauge, (Merz & Blöschl, 2009)

In Fig. 2.1 the location of the hydroclimatic regions are shown; the focus of this thesis is on the "Northern lowlands" and on the "Eastern lowlands". The "Eastern lowlands" are located in east and northeast territory of Austria and it is the driest part. The catchments in this region are mainly flat and the geology is of tertiary and quaternary origin. The "Northern lowlands" instead, are located in the Northwest part of Austria and it has a barely higher rainfall but the distribution of the runoff coefficient can be considered the same.

The eastern part of Austria is characterised by the Pannonian climate which behaviour produces warm and dry summer and cold winters without significant

snowfall. This behaviour is fundamental for the study because snowfall and glacier affect the runoff coefficient.

The work of Merz and Blöschl (2009) explains the dependency of the runoff coefficient with different catchment attributes. Regarding the two regions taken into account, the correlation of the runoff coefficient and the catchment elevation seems not being relevant. In these regions also the effect of snow and glaciers, soil depth, vegetation cover and soil slope on the runoff coefficient behaviour is lower.

Merz and Blöschl also analysed the controls on the temporal variability finding that event rainfall depth is not a major control on the runoff coefficient but duration can be a driver of an high runoff coefficient. In fact, events with larger duration tend to generate an higher runoff coefficient.

This research points out also the strictly dependence of the runoff coefficient to the event antecedent soil moisture for both the regions considered but the event rainfall is not able to alters the soil moisture state because of the dry condition of the soil.

Austrian runoff coefficients are distributed according to a Beta distribution (Merz et al., 2006) through which it is possible to classify the catchments. Merz analysed runoff coefficients of all the events in each Austrian catchments, there are six different regions based on the Beta distribution parameters.

This classification exhibits six regions instead of five and they are distributed in a different way, Fig. 2.2.

For what concern the two regions considered in the study, the "Northern lowlands" and the "Eastern lowlands", the average runoff coefficient is very low, due to the dry climate of the regions. As we can see in Fig. 2.3, the two catchments (Zwettl and Schützen) representative of the two dry regions of Austria exhibit a direct runoff much smaller than in the Lunz catchment that is located in an Alpine region.

What Merz found is that in these regions there is a small correlation between rainfall and runoff coefficient. During large events the runoff coefficient tends to be large, but only in rare case it is possible to find a very large runoff coefficient because most of the rainfall infiltrates during an event.

In those catchments the runoff coefficient differs significantly. For the two wet catchments it has not been found any runoff coefficient with a value lower than

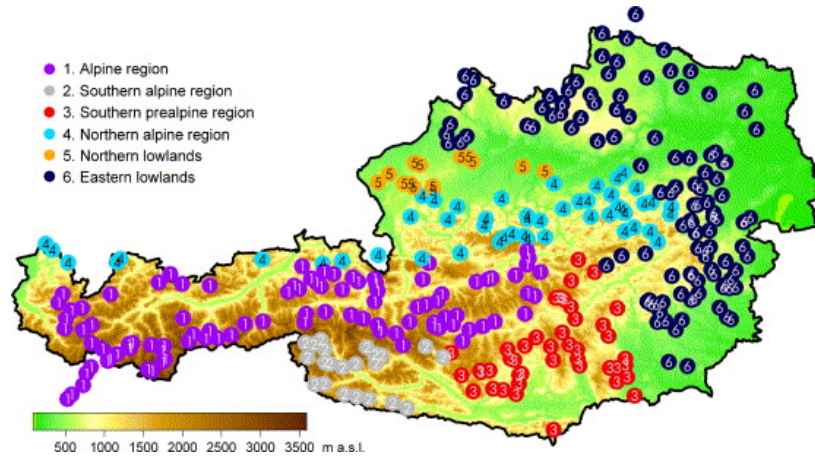


**Fig. 2.2.** Location of regions with similar distribution functions of event runoff coefficients. Numbers have been plotted at the location of each gauged catchment and refer to the group (Merz et al., 2006).

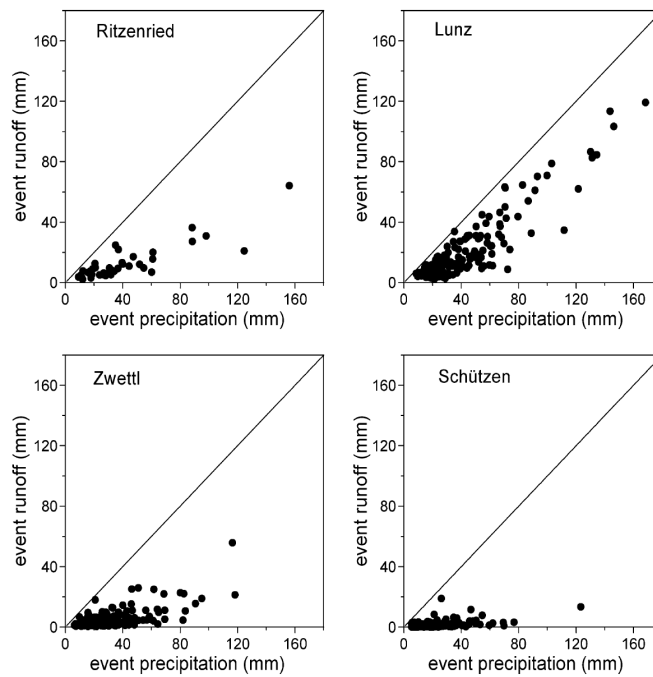


**Fig. 2.3.** Event runoff depth vs. event rainfall (including snowmelt) for four catchments in Austria. (a) Ritzenried/Pitze (220 km<sup>2</sup>); (b) Lunz am See/Ois (117 km<sup>2</sup>); (c) Zwettl/Kamp, (622 km<sup>2</sup>); (d) Schützen am Gebirge/Wulka (384 km<sup>2</sup>).

0.1 while the 90% quantiles of the runoff coefficient distribution of the other two catchments is 0.46 and 0.18 respectively.

## 2.2 Role of the soil moisture

Soil moisture can be extremely hard to be measured at a catchment scale, thus mean annual precipitation can be a surrogate of the wetness conditions and it can be used to explain the hydroclimate situation of a catchment.

Soil moisture can play a relevant role in the runoff generation.

Generally, in the orographic rainfall regions the magnitude of the floods tend to be higher because of the persistent high runoff coefficient caused by the high annual rainfall amounts and so of the high soil moisture level (Breinl et al., 2021).

Merz and Blöschl (2009) found out that there is a correlation between runoff coefficient (analysing events of Austrian catchments) and mean annual precipitation if we consider only those catchments not glaciated, because it can affect the runoff generation process and thus the runoff coefficient.

Combination of extreme storm events and high soil moisture can obviously lead to an extreme flood event. This condition does not happen on every catchment in which extreme storms are shifted from extreme flood events instead (Sivapalan, Blöschl, Merz, & Gutknecht, 2005).

The antecedent soil moisture of an event still seems to be the main driver of the extreme flood events, but they can not be necessarily related to extreme rainfall events.

Sivapalan et al. (2005) found that soil moisture differs within seasons because it is affected by seasonality of rainfall and evapotranspiration, and thus may have an indirect effect on the magnitude of the flood peaks.

Moving away from Austria, there are other case study in which the disparity between the dates of precipitation and the flood event is a clear sign that other mechanisms control the runoff generation.

Even in the U.S (Berghuijs, Woods, Hutton, & Sivapalan, 2016) the soil moisture is one of the dominant driver of the floods for the majority of catchments, while in the catchments with a lot of snow, the snow processes control the flood generation and timing.

## 2.3 Duration of rainfall and flood events

Duration of the flood and rainfall events can differ within season and within geography due to the difference in the rainfall generation processes and catchment characteristics.

### 2.3.1 Rainfall duration

Rainfall intensity can be affected by the duration or they can be inversely correlated. In fact in Fig. 2.4 the scaling parameter  $\eta_p$  (explaining the change of intensity with duration, indicator for convective activity) is higher in the convective rainfall region, which means that the rainfall intensity tends to decrease with the increasing of the event duration.

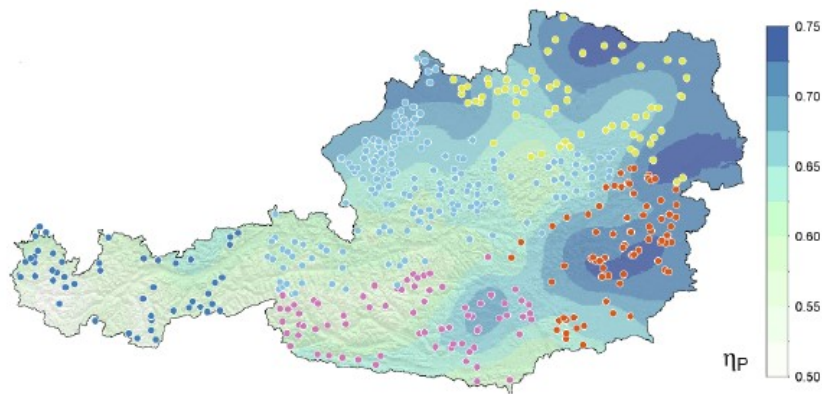


**Fig. 2.4.** Spatial pattern of the scaling parameter  $\eta_p$  used in Breinl et al. (2021) as one of the rainfall model parameters studied. Colored points represent the rain gauges inside the different hydroclimatic regions.

For catchments of a medium size (area around 130 km<sup>2</sup>) the majority of the events with an high runoff coefficient are produced by smaller but persistent rainfall events. In those catchments there is a correlation between runoff coefficient and event duration. This can also be seen in Fig. 2.5 that suggests that longer rainfall events but with lower intensity tend to have higher runoff coefficients.

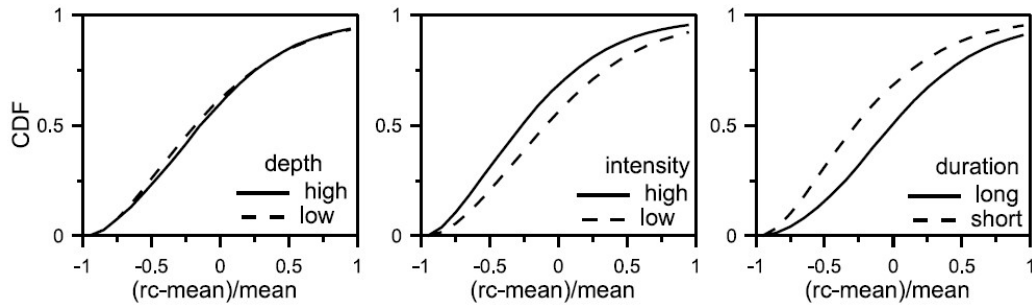


**Fig. 2.5.** Distribution function of event runoff coefficient deviates stratified by (left) small (dashed lines) and large (solid lines) event rainfall depth, (middle) lower (dashed lines) and high (solid lines) maximum event rainfall intensity, and (right) shorter (dashed lines) and longer (solid lines) rainfall duration (Merz & Blöschl, 2009).

### 2.3.2 Flood duration

Flood timescale is sometimes governed by catchment area because of the longer flow paths and river density. In Fig. 2.6 we can see that there is not a strictly correlation between flood timescale and catchment area but from Fig. 2.7, short flood events do not happen in small catchments.

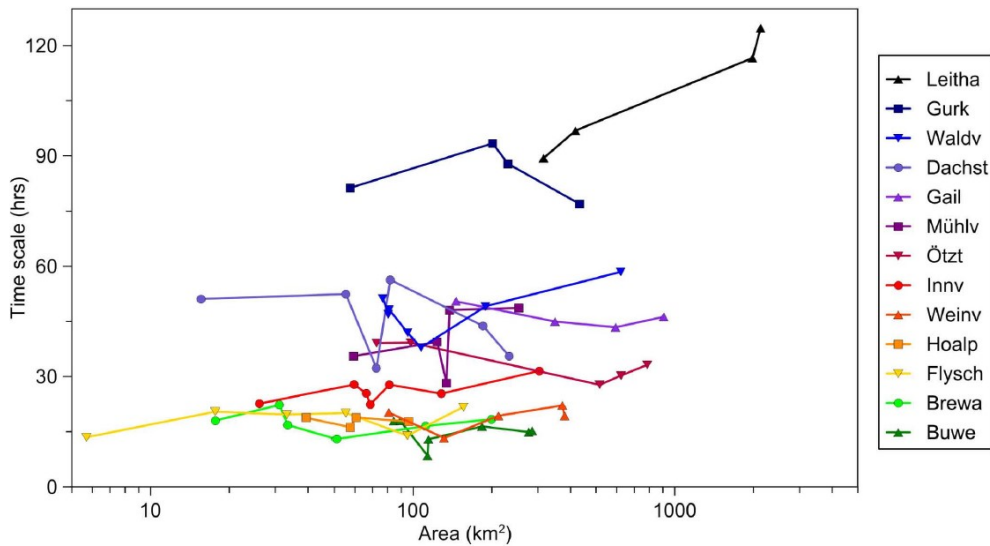


**Fig. 2.6.** Median of flood timescale for each catchment as a function of catchment area. Each line represent a studied hot spot in Gaál et al. (2012).

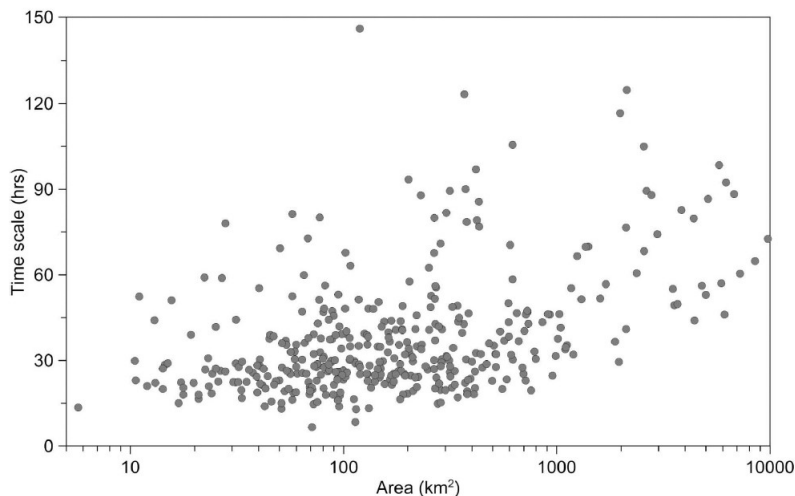


**Fig. 2.7.** Median of flood timescale in Austria plotted versus catchment area ( $\text{km}^2$ ), (Gaál et al., 2012).

Flood duration may be controlled also by soil moisture which is usually higher in spring because of the snow melt process and low evapotranspiration caused by the low temperature.

Higher values of soil moisture contribute to generate higher flood volumes and it may also be an explanation for the larger timescale of flood events.

### 2.3.3 Critical storm duration

Catchment response time is another catchment characteristic from which large floods may be generated.

Through some simulations, focused on finding the importance of storm duration in flood generation, Viglione and Blöschl (2009a) defined the importance of the rainfall duration with respect of the catchment response time.

Storm duration is considered critical when it is on the order on the catchment response time because it becomes crucial in the flood generation. When the storm duration has the same magnitude of the catchment response time, the flood generated by the storm is transformed into annual flood with higher probability.

Even with large runoff coefficient, flood events are associated with low return period if they are generated by storms with a duration very different from the catchment response time (Viglione et al., 2009b). This is the case showed in Fig.

2.8 in which, in the upper part of the graph, a lot of events have a low flood return period even if they are associated with a high runoff coefficient.

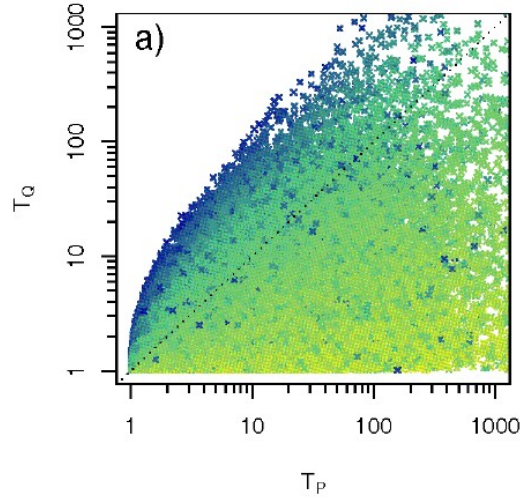


**Fig. 2.8.** Mapping of return periods obtained simulating 100 000 years of events. Events characterized by high runoff coefficients are dark-blue while low runoff coefficient events are represented in light-green (Viglione et al., 2009b).

## 2.4 Runoff coefficient distribution through Monte-Carlo simulation

Using a Beta distribution for the runoff coefficient, in Viglione et al. (2009b) the flood frequencies from rainfall has been derived with a Monte-Carlo simulation.

In the study, Viglione made an artificial world in which the processes are generated from a block rainfall and a linear catchment response. In the case of the block rainfall the aggregation level ( $t_{IDF}$ ) used to evaluate the return period of the rainfall is considered equal to the duration ( $t_r$ ) of the rainfall itself.

Through Monte-Carlo approach  $N$  years of rainfall events have been generated, then with the Beta distribution of runoff coefficient it has been possible to evaluate the runoff.

Assuming the runoff coefficient as a random variable, it varies independently from the storm characteristics taking more into account the antecedent soil moisture as a driver factor in the runoff generation (Merz et al., 2006).

## 2.4. Runoff coefficient distribution through Monte-Carlo simulation

As it can be seen in Fig. 2.9, different systems with different distributions of runoff coefficient produce different events return period. In fact in the dry system, events with very high runoff coefficient (meaning an high return period) are rare but they can occur. On the contrary in a wet system, events with high flood peak (meaning an high runoff coefficient) are frequent, resulting in a flood return period not so high.

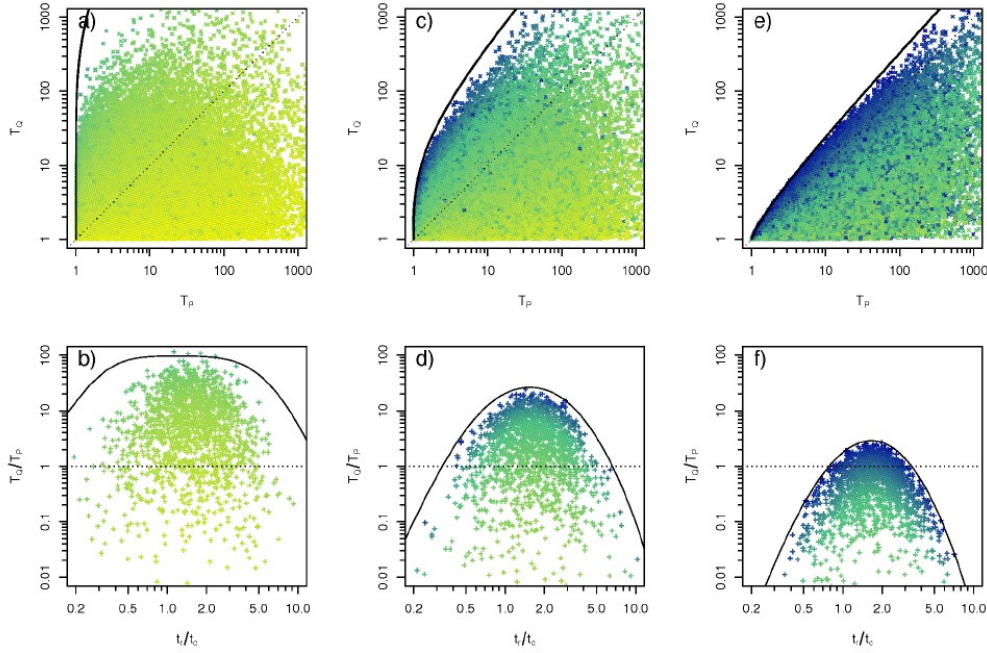


**Fig. 2.9.** Relationship between rainfall return periods  $T_P$  and flood return periods  $T_Q$  for beta distributed runoff coefficients  $r_c$  independent from the rainfall events. The three upper Panels (a), (c) and (e) represent the mapping of  $T_P$  vs.  $T_Q$ . The crosses are obtained by Monte- Carlo simulations (100 000 years). The envelope curves (continuous lines) are calculated analytically. The three lower Panels (b), (d) and (f) represent one horizontal slice ( $T_Q = 100$  years) of Panels (a), (c) and (e) respectively in terms of the ratio of return periods  $T_Q/T_P$ . The parameters of the beta distribution are: Panels (a) and (b) – Dry system with average runoff coefficient  $\delta_c = 0.1$  and variance  $\sigma_c^2 = 0.009$  ( $CV_c = 0.95$ ); Panels (c) and (d) – Wetter system with  $\delta_c = 0.3$  and  $\sigma_c^2 = 0.038$  ( $CV_c = 0.65$ ); Panels (e) and (f) – Very wet system with  $\delta_c = 0.7$  and  $\sigma_c^2 = 0.022$  ( $CV_c = 0.21$ ) (Viglione et al., 2009b).

Considering seven different systems, the runoff coefficient  $r_{1:1}$  for which  $T_P = T_Q$  have been calculated to analyse which one should be used in an engineering prac-

tice.

The runoff coefficient  $r_{1:1}$  has low values for a dry system and high value for a wet system and it varies with the return period considered, Fig. 2.10.

In panel (b) of the Fig. 2.10, it is possible to observe that the probability of non-exceedance of the runoff coefficient  $r_{1:1}$  with respect of all the runoff coefficients of all events, is around 0.9 for all the wetness conditions.

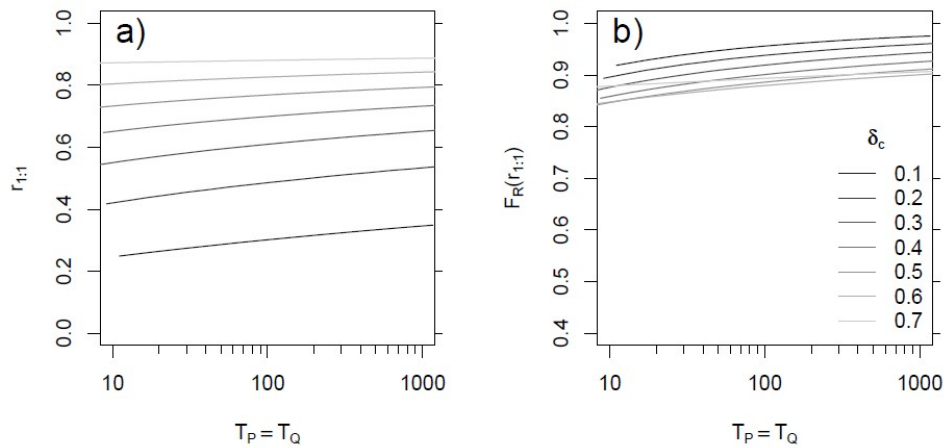


**Fig. 2.10.** Runoff coefficients  $r_{1:1}$  that give a 1 to 1 correspondence between rainfall and flood return periods plotted against return period. Panel (a) – Runoff coefficient  $r_{1:1}$ ; Panel (b) – Non-exceedance frequency of  $r_{1:1}$  on the parent distributions of  $r_c$ . The parent beta distributions correspond to the seven wetness conditions labeled with seven different runoff coefficients (from dry to wet systems) (Viglione et al., 2009b).

A complete and exhaustive data set is crucial for any analysis of flood risk because it needs to be coherent within the region analysed. The data set should comprehend both climate and catchment characteristics together with hydrologic information, covering the entire region with high detail.

In this chapter, the information that the data set could give are explained. The data set includes information regarding topography and catchment boundaries and hydrology such as flood data and rainfall data.

### 3.1 Starting data set

The study is set in Austria using data for a period of about 30 years, from 1985 to 2015. Rainfall data and stream data were available thanks to the database of Technical University of Vienna that has data record from more than 400 stations, as we can see in Fig. 3.1. In the figure, there are all the rain gauges and stream gauges within Austrian borders, where stream stations are represented as a red square while the rain gauges with a water drop icon. Most of them record hourly data (for rainfall gauges) and fifteen data (for stream gauges); regarding rain gauges, only some of them record daily data. All of the rain gauges in the Figure, together with other stations outside Austria, non reported here, are used for the rainfall interpolation.

#### 3.1.1 *Rainfall interpolation*

To utilise a more detailed and relevant rainfall information, hourly precipitation were spatially interpolated with the inverse distance-weighting method (Merz et al., 2006).

The rainfall data were interpolated with each catchment boundaries to ob-

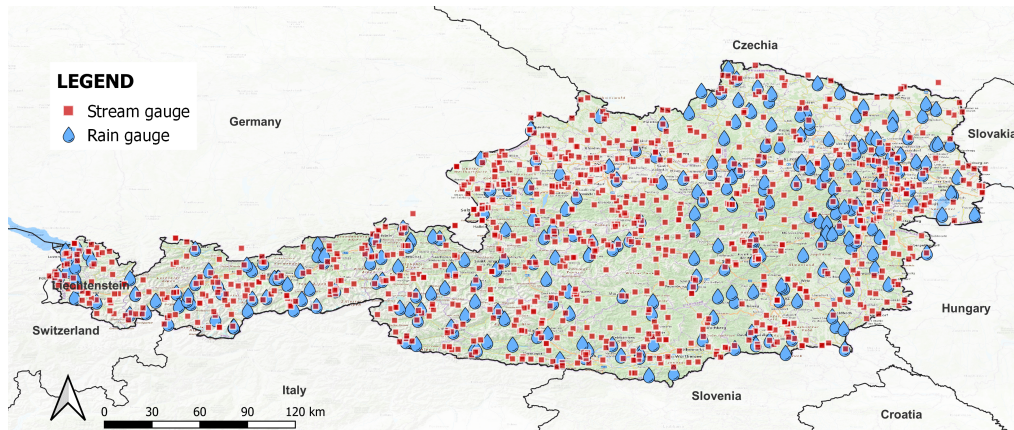


**Fig. 3.1.** Available data set for the entire Austria with Stream gauge and Rainfall gauge location.

tain hourly catchment precipitation. To achieve the interpolation, random and equidistant points were generated inside each catchment and values for each point are estimated based on their distance from known points that are the rain gauge stations. Points that are closer to known values will be more influenced than points that are further away. Hourly catchment precipitation is obtained as average of the values of each generated point within catchment boundaries.

This method tends to give some biased values, especially for rain gauges that are located in valleys because of the elevation effect that produces underestimation on precipitation values. In order to correct the bias, the mean annual precipitation were compared with SPARTACUS database.

Solid precipitation will not contribute to the direct runoff but snow melt from a previous precipitation could add a relevant amount of water to the runoff. To account for this effect, a daily water balance model can be used to correct the rainfall information. Solid precipitation can bias the values but it is relevant only in the Alpine regions while in the Lowlands, where we carried out the analysis, this phenomena is negligible because the snow fall is very rare and with a low magnitude.

### 3.1.2 *Runoff data*

For all the stream stations in Fig. 3.1, fifteen minutes data are available and they were aggregated to obtain hourly runoff data.

Discharge data were screened and those with relevant anthropogenic impacts were removed. Also catchments with large area are not considered because of the higher variability of the runoff coefficient (Merz et al., 2006).

## 3.2 Area of study

Among all the stations available in Austria, only the territory of East Austria are considered because the influence of the solid precipitation is negligible.

For all the stream stations analysed in the thesis, viewable in the map in Fig. 3.2, stream data and rainfall data from 1985 to 2015 were available.

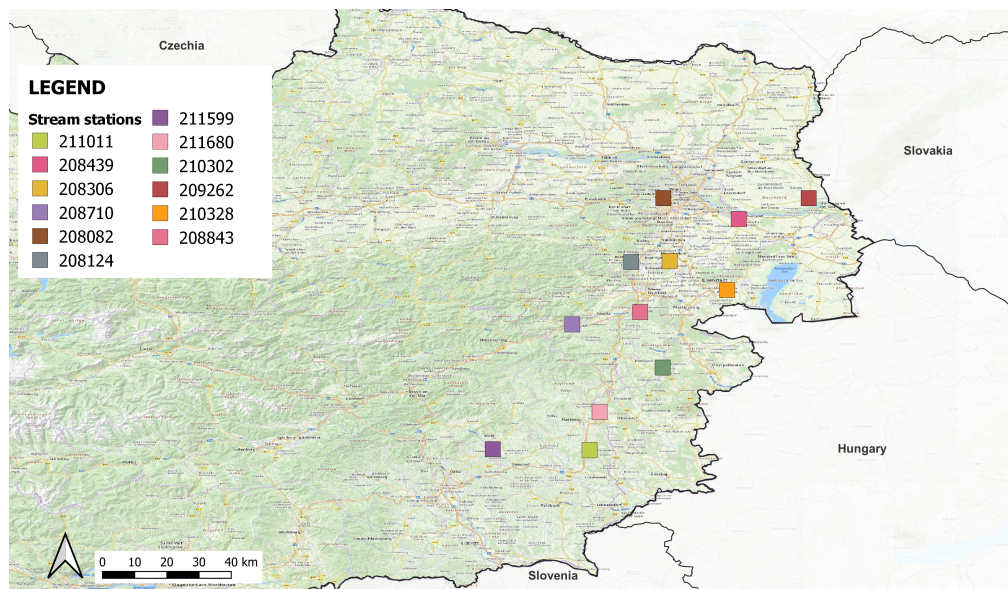


**Fig. 3.2.** Location of the stream gauges considered in the thesis. Only catchments with an area between 80 and 600 km<sup>2</sup> are considered.

Catchment characteristics such as mean elevation and area are reported in Table 3.1; most of the catchment characteristics available were taken from the TU Wien database.

The catchments selected have an area ranging from 80 to 600 km<sup>2</sup>. Smaller catchments that were available in the region were discarded because of the possible uncertainty that can occur with the rainfall spatial interpolation. In larger catchments, the variability of runoff coefficient was assumed to be large, so also those catchments were discarded.

**Tab. 3.1.** Information of the catchments involved in the study. This table describes the characteristics of the stream station reported in Fig. 3.2. The MAPs are calculated from the stream data available.

id	Stream Gauge/Stream	Elevation (m. a.s.l.)	MAP (mm/y)	Area ( $km^2$ )
211011	Waltersdorf in Oststeiermark/Safenbach	283	762.58	343.4
208439	Fischamend(Rohrbrücke)/Fischa	152	775.23	534.9
208306	Tattendorf/Piesting	221	891.46	305
208710	Gloggnitz(Adlerbrücke)/Schwarza	435	1177.27	472.2
208082	Kennedybrücke/Wien	183	747.89	199.4
208124	Hirtenberg/Triesting	277	856.99	287.3
211599	Mitterdorf an der Raab/Raab	398	940.22	183.7
211680	Hammerkastell/Lafnitz	365	916.82	285.5
210302	Kirchschlag in der Buckligen Welt/Zubernbach	408	849.29	113.6
209262	Engelhartstetten/Rußbach	138	476.45	497.8
210328	Trausdorf an der Wulka/Wulka	143	700.67	235.9
208843	Erlach/Pitten	307	887.72	412.9

For each catchment it is possible to represent the entire data set for both rainfall and stream flow in a single plot that can be used in the next step, Fig 3.3. The data set for each single catchment used can be found in the Appendix B.1.

The data set constitute the total duration series and need to be screened from worthless information to reduce the computational time.

In the graph the hourly stream records are reported as black line and the unit of measurement are mm/h to be compared with the precipitation. The mm/h unit is a specific discharge, in fact the actual data are recorded in  $m^3/s$ ; they are transformed in mm/h for two reasons: (i) to be in the same unit of precipitation data so they can be compared and (ii) they are divided by the area of the catchment to obtain the specific discharge so the catchments can be compared among them self.

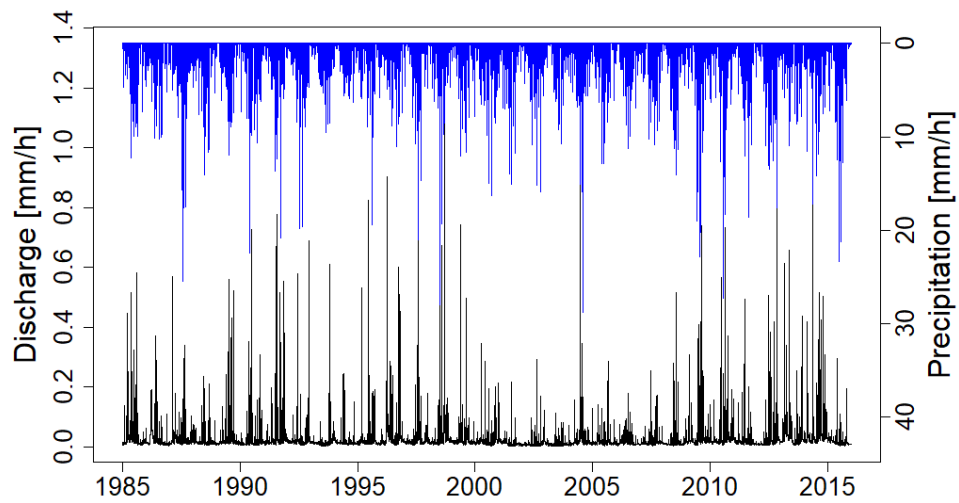


**Fig. 3.3.** Total duration series for a single catchment. The black line represents runoff data while the blue bars represent rainfall series



# Methodology

## 4.1 Introduction

The design storm procedure idea is to estimate a flood of a selected return period from *intensity-duration-frequency* curves for the site of interest. It is important, in order to avoid underestimation of the flood magnitude, to perform the frequency analysis for each catchment, obtaining a return period for each intensity and duration.

Then, the hydrological procedure consists in the transformation of the designed storm to a flood hydrograph with an event based runoff model that needs to be calibrated for the catchment of interest.

Calibration of the model in this type of process, as we will see in the following paragraphs, is fundamental because runoff is affected by many factors that are different for each catchment.

## 4.2 Statistical analysis

Considering that hydrologic data are the only source of information upon which quantitative hydrologic investigation are generally based, their measurement have been continuously expanding and resulting in ever-increasingly large amounts of sampled data.

Because of the stochastic nature of the natural hydrologic phenomena, hydrologic data can suitably be expressed in statistical terms and be treated with probability theories.

One of the most important problems in hydrology is the interpretation of past records in terms of future probability occurrence of the phenomena and the procedure that deals with this problem is the so called probability analysis.

### 4.2.1 General terminology

In statistics, the whole data set is called *population*, or universe. A portion of a population may have one or more characteristics associated with them and they are depicted as *variable*. A single observation of the data set or a single value of the variable is known as *variate*.

Variables may be obtained by an experiment or by collecting data, in hydrology the collection of variables can be done by instrument such as rain gauge and the result is called *random variable*. Random variables are of two kinds: *discrete* or *continuous*. The discrete variable has a finite sample space, while the sample space of the continuous variable can be an interval.

For discrete random variables, the number of occurrence of a variate is generally called *frequency* and if it is plotted against the values of variate itself it is possible to obtain the *frequency distribution*.

When the number of occurrences of a variable is divided by the total number of occurrences, the *probability* of the variate can be obtained. Plotting the probability, instead of frequency, against the values of the variate, it is possible to obtain the *probability distribution*.

Generally, the hydrologic data are presented in chronological order, Fig. 4.1, they are available for a certain period of time and they are represented by their magnitude in an arbitrary unit. Because of the large amount of data and because many of the original data have no particular significance for the analysis, they are usually screened according to the magnitude in order to save labor and time in the analysis. As we can see in Fig. 4.2 only the data inside flood events are considered as relevant and this data set is called *partial-duration series*.

The average interval of time which magnitude can be equaled or exceeded by an event is known as *return period* or *recurrence interval* and can also be expressed as the inverse of the average frequency of occurrence.

### 4.2.2 Frequency analysis

The cumulative probability of a distribution can be represented graphically on a probability paper which is designed for the selected distribution. Generally the probability paper is a graph in which there is the probability or the recurrence interval on the abscissa and, the value of the variate in a certain scale on the

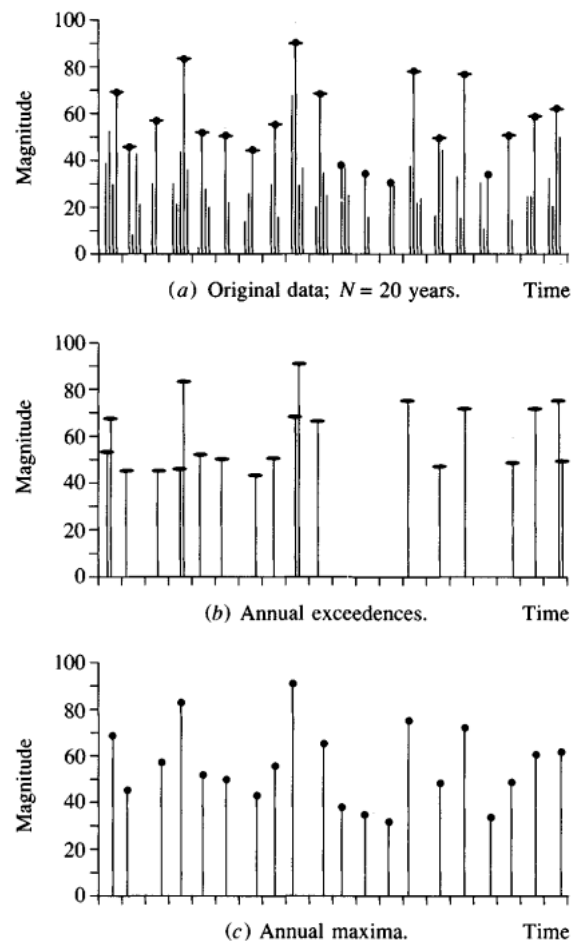


**Fig. 4.1.** Example of hydrologic data arranged according to the time of occurrence (Chow, 1964).

ordinate.

### 4.3 Events data

As explained in the *chapter 4.2.1*, it is more practical to analyse the partial duration series instead of the whole data set since a lot of records have no useful information.

In this chapter i resume the main steps of the event separation code as a digital filter. The code compiled in , can be found in the Appendix A.2.

The identification of runoff events consists in three different steps: base flow

separation, event separation and attribution of rainfall to events.

Base flow separation consists in a division of streamflow time series between quick flows and base flows. The events are then identified with their start and end time according to a separation threshold. Finally, rainfall events are attributed to the identified runoff events.

### 4.3.1 Base flow separation

The event runoff coefficient relates to direct runoff or quick flow only, so it is necessary to separate it from the baseflow.

Direct runoff accounts for rainfall that contributes immediately to streamflow during an event, while the base flow, moving slower, contributes to streamflow with a significant delay.

To process the data an automatic method of base flow separation, regarding the Maxwell and Chapman filter (Chapman and Maxwell (1996)), were used.

The Chapman and Maxwell filter can be expressed in the form:

$$q^b(t) = \frac{a_2}{2 - a_2} q^b(t - \Delta t) + \frac{1 - a_2}{2 - a_2} q(t), \quad q^b(t) \leq q(t) \quad (4.1)$$

$$a_2 = e^{-\frac{\Delta t}{k_2}} \quad (4.2)$$

$$q^d(t) = q(t) - q^b(t) \quad (4.3)$$

where  $q^b(t)$  is baseflow,  $q(t)$  is runoff and  $q^d(t)$  is direct runoff at time  $t$ .  $\Delta t$  is the sampling interval of 1 hour in this study. Parameter  $a_2$  is a function of the storage parameter  $k_2$ .

The parameters of the filter used in this study derive from the manual inspection previously done for the Austrian catchments by R. Merz (Merz et al. (2006)) and they have been set in the code in the Appendix.

### 4.3.2 Event separation

After the baseflow separation, streamflow time series were screened to identify runoff events.

The event separation allows to identify the start and the end of an event by an iterative procedure (Merz et al. (2006)). For each peak flow, the start and the end of an event is searched within a given time period by finding the time when the direct runoff becomes lower than a given threshold, which depend on the direct runoff at the time of the peak value. If no starting point is found, the search is repeated increasing the time period and the threshold.

### 4.3.3 Attribution of rainfall events

For each event that has been extracted by the previous step it is necessary to attribute the hourly rainfall depth, the hourly discharge data and eventually the snow melt data.

At the end of the separation we can retrieve an hydrograph and a hyetograph for each single event, as shown in Fig. 4.2; in the graph also the baseflow can be seen.

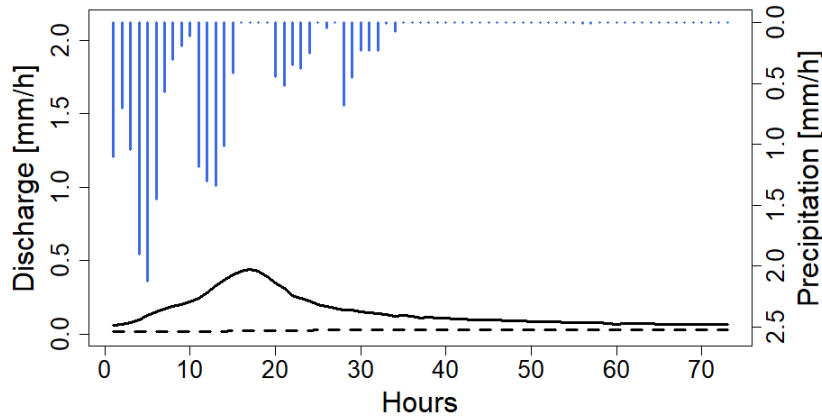


**Fig. 4.2.** Hydrograph and hyetograph for an identified event with Chapman and Maxwell filter. The dotted line represents the baseflow, the solid line represents the observed runoff and the blue bars represent the event rainfall.

For each catchment it has been possible to extract a huge number of events, Fig. 5.1, that can be characterized singularly by the factors described in the following paragraph.

## 4.4 Catchment and event characteristics

Based on the set of identified events i analysed the different dynamics of the possible generation processes of runoff coefficients on different temporal scales: variations between events and seasonality, analysing each catchment once at a time. Furthermore, selecting catchments in a single hydrologic region, it is possible to conduct the analysis combining all the events of all catchments together.

To depict the various behaviours, i considered different possible drivers that could give an insight on the processes of runoff generation and on their variability.

First of all it is important to distinguish among event characteristics and catchment characteristics, the former can be evaluated starting from event rainfall and event runoff while the latter can be described as environmental or topographic characteristics.

### 4.4.1 *Event characteristics*

Three possible drivers of the runoff generation have been extracted through the computation of event runoff data and event rainfall data. Starting from the initial date of the event, the rainfall volume (I), the direct runoff volume (II) and the duration (III) of the event have been calculated.

(I) The rainfall volume is the sum of the hourly rainfall within the event starting and ending dates and it can be expressed as mm.

(II) The direct runoff volume can be considered as the total volume of water that comes to the stream gauge; the amount of baseflow is not accounted in the direct discharge volume (the two variables are considered separated, as previously shown in Fig. 4.2). This volume can be considered as a specific volume; this allow the comparison between all the catchments.

(III) Duration is the total amount of hours of the event within the runoff event period.

Other characteristics have been considered such as peak flow and rainfall peak intensity.

## 4.5 Definition of storm return period

The return period of a storm can be expressed using the IDF curve (Intensity – Duration – Frequency curve) that relates the intensity of the storm with its duration and frequency of occurrence. For each duration selected, the annual maximum rainfall intensity is extracted from historical rainfall records. Then frequency analysis is applied to the annual data extracted, obtaining a return period for each intensity and duration.

### 4.5.1 Extraction of the annual maximum rainfall intensity

The extraction of the annual maximum rainfall intensity can be performed moving an averaging window of different widths according to the duration selected. The “duration” in the procedure differs from the storm duration and it is called aggregation level. For each year of the record, the maximum average intensity for each aggregation level is extracted.

### 4.5.2 Frequency analysis of the annual rainfall data

Frequency analysis is obtained by the plotting position on a probability paper and then by the curve fitting to the plotted points (Chow (1964)).

Plotting positions can be considered as the estimation of the probabilities of the cumulative distribution function and can be achieved with different formulas, the one used in this study is the Gringorten formula.

$$T = \frac{N + 0.12}{m - 0.44} \quad (4.4)$$

where  $N$  is the total number of items and  $m$  is the order number of the items arranged in descending magnitude, thus  $m = 1$  is for the largest item.

The Gringorten formula (4.4) can be modified as follow, in order to obtain also return period lower than one year (Fig. 4.3). This is because the IDF curve is not made on the annual peak but on all events. The new Gringorten formula is:

$$T = \frac{N + 0.12}{m - 0.44} \cdot \frac{1}{n} \quad (4.5)$$

where  $n$  is the average number of events per year.

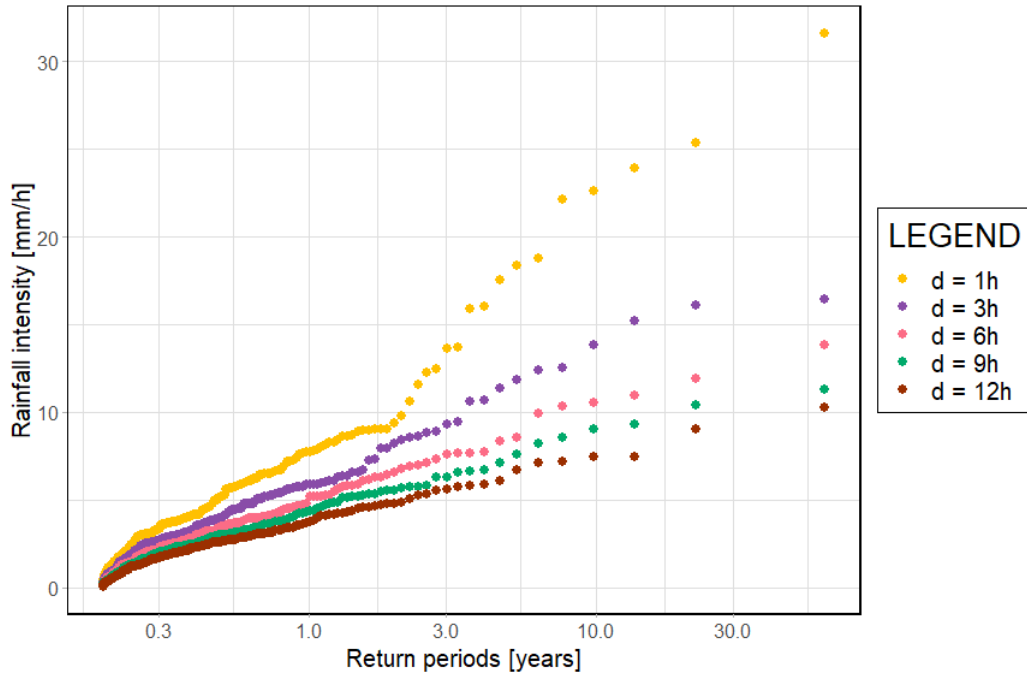


**Fig. 4.3.** Example of IDF curve for each time window within each single event.

After the hydrological data are plotted on a probability paper, a curve may be fitted to the plotted points.

**Generalized Pareto** The curve that has been fitted to the IDF curve is the Generalized Pareto whose parameters have been calculated with the *method of moments*. In this study the GEV distribution could not be used because it is appropriated only when the data consist of a set of annual maxima.

It can be assumed that the events data are as POT (*Peak-Over-Threshold*) values; the GP distribution is the most suitable distribution for this type of data.

As it can be seen in Fig. 4.4, the GP distribution is very suitable for the lower values of rainfall but they influence the behavior of the curve and the higher values are not well represented. More details of the Generalised Pareto distribution can be found in the Appendix A.1.

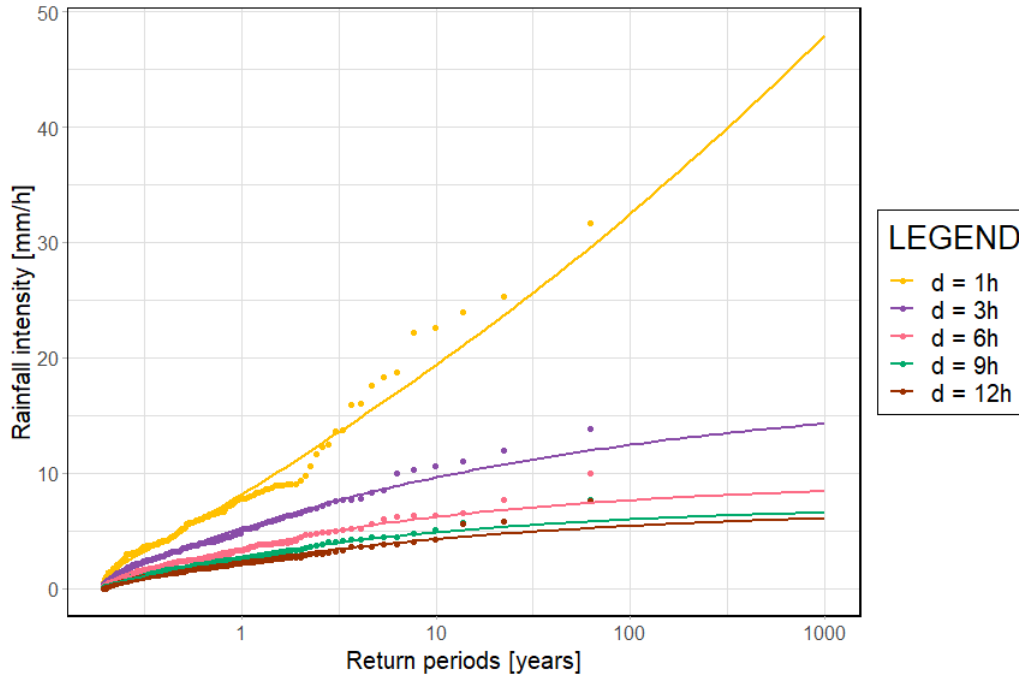


**Fig. 4.4.** Example of IDF curve for each time window within each single event. Generalized Pareto distribution has been fitted to each single set of data.

### 4.5.3 Frequency analysis of the event runoff intensity

The same procedure for the extraction of the return period of each single event has been applied for the runoff data.

Applying the Gringorten formula (4.5) to the event runoff data, it is possible to represent each single event on a probability paper.

In hydrology, the averaging window used for the construction of the IDF curve is not usually applied to the runoff data. In this case, the Gringorten formula has been applied only on the event maximum runoff intensity (also represented with an averaging moving window of 1 hr) and then fitted with a frequency curve.

As rainfall event data, event runoff data can be considered as POT values because the data analysed include all the events extracted that have a frequency lower than a single year.

Because of this, also in this case, the GEV cannot be used (GEV is usually used for annual data) but it is necessary to fit the GP distribution to the plotted point in order to better represent the tail of the distribution.

All the QDF curve for each single catchment are reported in the Appendix B.3.

## 4.6 Seasons

Due to the different types and characteristics of the processes of precipitation and climate during the year, it is important to distinguish those process characteristics and if there is a special pattern or behaviour.

Usually the seasons are four and they are divided in: Winter from December to February (DJF), Spring from March to May (MAM), Summer from June to August (JJA) and Autumn from September to November (SON).

The events are classified by the seasons based on the first day of the event itself.

The analysis based on the different seasons will give an insight on the future analysis that could be done to improve the results. The analysis that could be found in the chapter 5.8, uses the same graphs of the other chapter but they are improved with the season subdivision.

It will be used also a box plot to better explain the differences among the seasons. The box plot is a type of graph useful to represent a distribution of values, its shape and if there are some outliers. The box plot, also described in Fig. 4.5, it is used to better illustrate the distribution because it, somehow, excludes the outlier. In fact, the Interquartile Range (IQR) is used to design the length of the plot and also to decide the minimum and the maximum value. The ends of the box plot are either a 1.5 times the IQR value and the maximum and minimum data values excluding the outliers.

The box plot will be used for the comparison of the runoff coefficient among the seasons being interested in the median value at this level of the study.

## 4.7 Spearman correlation

Spearman coefficient can be useful to measure the level of correlation between two variables. The Spearman correlation test the strength of a monotonic association of a paired variables.

The coefficient, identified as  $\rho$ , can assume a value between -1 and +1 in which -1 means a perfect negative association, 0 means no correlation and +1 means a

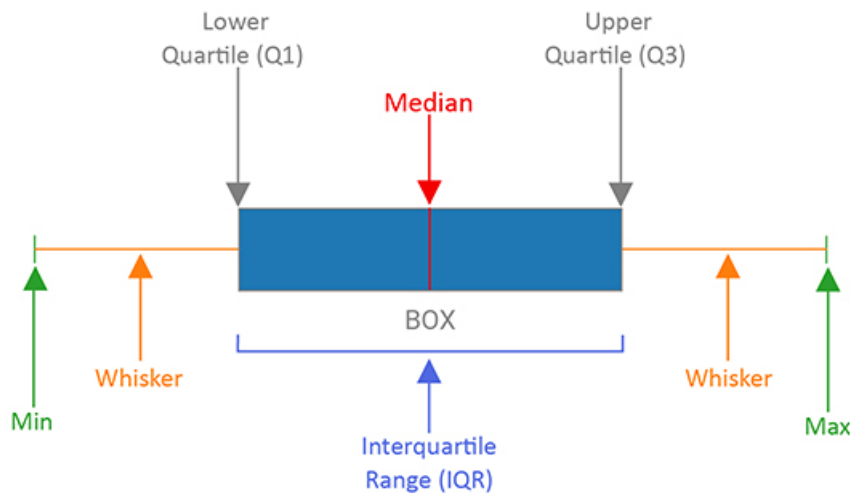


**Fig. 4.5.** Description of a box plot with its quartiles. The Lower Quartile represents the 25th percentile of the distribution and the Upper Quartile represents the 75th percentile of the distribution.

perfect positive correlation. The closer of  $\rho$  to one the stronger is the correlation.

The problem that can arise with the Spearman correlation analysis is that a value equal to zero does not mean that there is not a correlation but it means that there is not a monotonic correlation.

The correlation test is implemented in  $\mathbb{R}$  with the command `cor.test` which uses the equation to evaluate the level of the correlation.

$$\rho = 1 - \frac{6 \sum d_i^2}{n(n^2 - 1)} \quad (4.6)$$

In this thesis the Spearman correlation coefficient will be used to understand from which flood characteristic the runoff coefficient is influenced.



# Results

## 5.1 Events extracted

Using the Chapman and Maxwell filter, all the events are extracted from the runoff and rainfall data. For each single catchment a large number of events have been selected, Fig. 5.1.

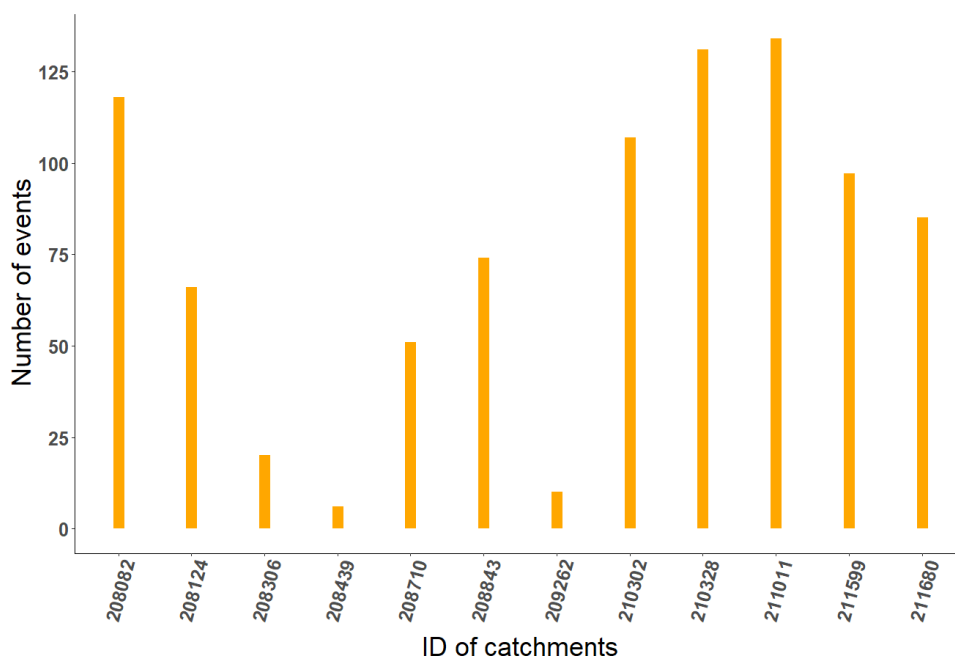


**Fig. 5.1.** Number of events extracted for each single catchment.

In Fig. 5.2 the events identified are overlapped to the runoff and precipitation data set used. In this case the filter identified very precisely the start and the end of the events. In the graph the dotted line represents the baseflow obtained through the base flow separation code, the solid line represents the runoff recorded

by the stream station while the bold line represents the events depicted by the event separation code. The blue bar represents the precipitation obtained with the spatial interpolation, therefore it is not the precipitation recorded by a rain gauge but it is an average rainfall within the catchment boundaries.

Because of the large number of parameters required by the event separation code, it is difficult to calibrate the model to recognise the start, the end and the multi peak in the runoff event. Some of the events that are small are not depicted and some events have not the right start or end. This inconvenient can be neglected for the analysis of a few catchments in which, in any case, all the extreme events are identified. It has also not been adjusted because it is a very time consuming procedure and the result will not be so different.

## 5.2 Plotting position and IDF curve

The Plotting position using the Gringorten formula is a valid method to retrieve the return period of the events, specially for the POT values.

All the results that will be presented here use the return period values obtained with the empirical formula and not with the fitting curve. This assumption entails that the maximum return period is only a function of the size of the starting data set. For most of the site analysed, this assumption does not affect the final results but for a few catchments, there can be an underestimation of the return period of the extreme events. However, using this method the median of the events are not affected.

In Appendix B.2, the IDF curve for each single catchment involved are reported individually. The curves report a return period lower than one year because of the POT values, showing also the magnitude of lower events. There are some catchments in which there have not been found a lot of events so only the extremes ones are reported, this is why there are only return period values higher than one year.

Another question about the analysis of the events only is that some extreme rainfall events are not depicted because the event separation is performed starting from the runoff data and then, the rainfall is assigned to the event itself. This problem may arise when an extreme storm event does not produce a runoff event, therefore the IDF curve should be assembled starting from the annual maxima.

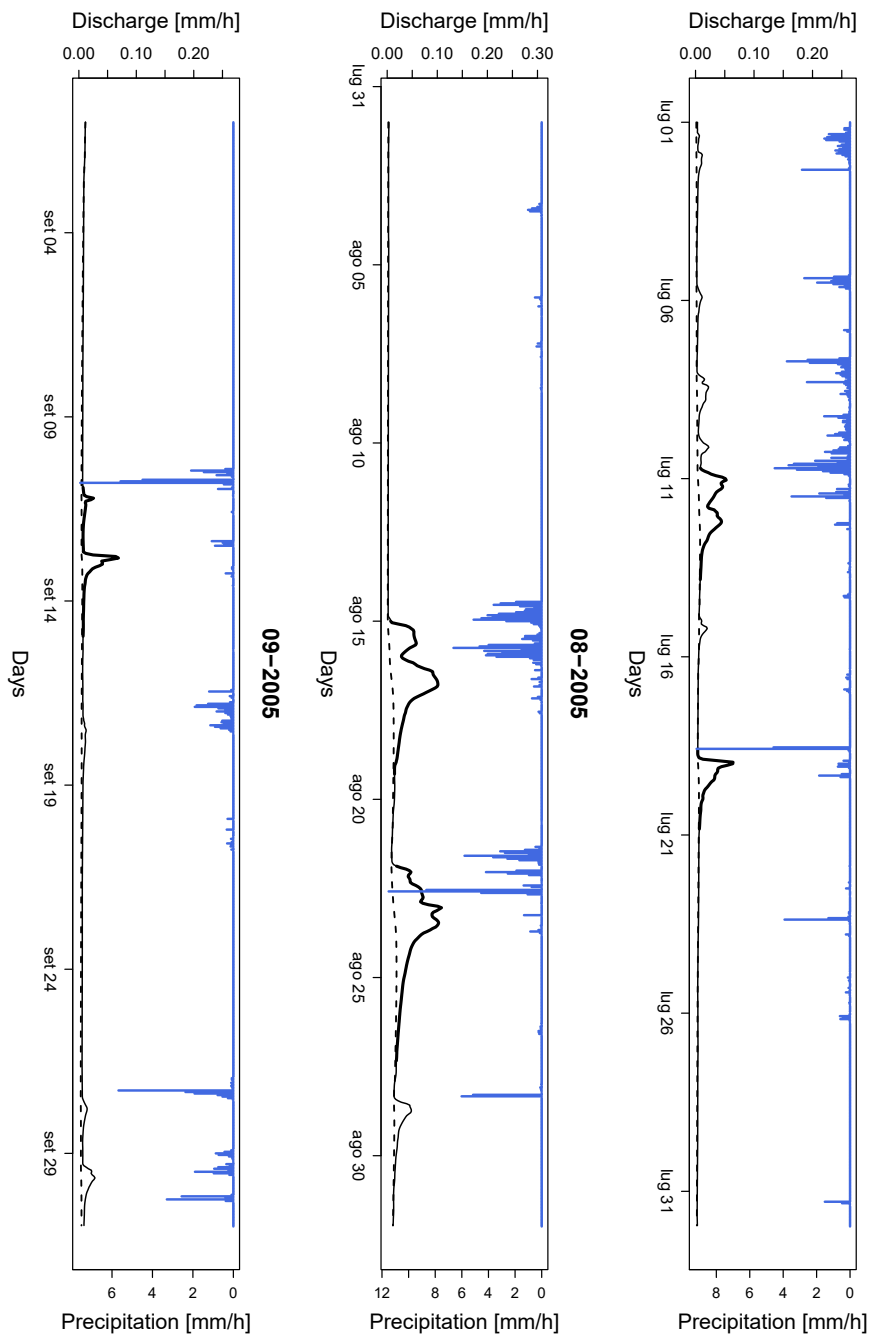


**Fig. 5.2.** Example of three hydrograph and hyetograph extracted, representing three months in which some events are depicted

The annual maxima have been extracted and used to build a stand alone IDF curve (not reported in the thesis) to prove the quality of the IDF event based. The return period retrieved from the annual maximum values are aligned with those event based so it has been decided to continue the analysis only with the event data.

### 5.3 Runoff return period

Based on the events extracted, it has been possible to evaluate the return period of the quick flow using the Gringorten formula. The procedure and the assumptions have been the same used for the rainfall analysis. Also in this case the return periods that will be used come from the empirical method and not from the fitted curve.

All the graphs regarding the evaluation of the return period together with the GP distribution for each single catchments are reported in the Appendix B.3.

### 5.4 Runoff regime

The runoff regime can be visualized by studying the events runoff volume and the events rainfall volume, putting them in contrast.

The runoff volume (represented as runoff depth) can be plotted against the rainfall volume (in terms of rainfall depth) for each event extracted. Each point stands for a single event and it is coloured according to its runoff coefficient.

In Fig. 5.3-5.4 it is possible to observe the different runoff regimes of all the catchments analysed. The physiographic and hydrological characteristics of the catchments are shown in Tab. 3.1.

All the catchments are located in a dry region in the East and North East of Austria and all of them are dominated by a convective rainfall; they have a similar behaviour in the hydrological regime but there are some differences here reported.

The Gloggnitz (n° 208710) is the catchment with highest Mean Annual Precipitation (1177 mm/year) among all the catchments analysed. From Fig. 5.3 it is possible to observe a different distribution of the events in fact, there is a tendency to have a higher runoff volume among all events depicted. This behaviour could be explained by the higher area of the catchment (472.2 km<sup>2</sup>) but mainly by the

highest MAP that could also generate the higher mean runoff coefficient around 0.38.

The Hirtenber (n° 208124) and the Kennedybrücke (n° 208082) are the other two catchments with the higher event rainfall volume. Despite this characteristic, only few storm events generate a runoff with high magnitude, but most of the flow volume still remain concentrated in the bottom part of the graph. Hence, also those catchments can be considered as dry catchments.

The highest runoff volume within all catchments are on the order of 50-70 mm even if the variability and the magnitude of the storms are very high.

Looking at the Fig. 4b in Merz et al. (2006), it is possible to observe a completely different behaviour in the Alpine region of Austria, in which the storm volumes can be considered of the same amount of the lowland region but the runoff volumes is almost twice as lowland catchments.

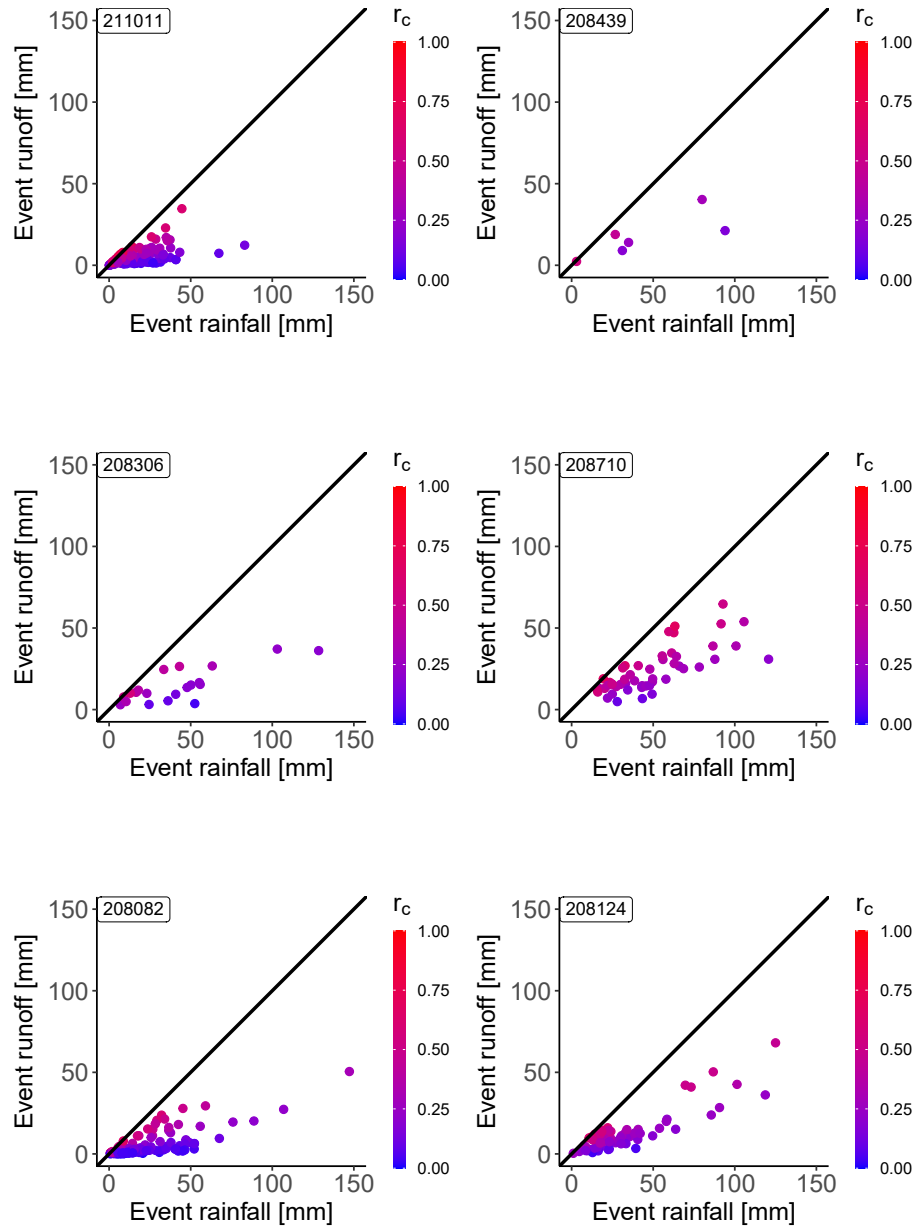


**Fig. 5.3.** Event runoff depth vs. event rainfall volume for all the catchments analysed. The plots are divided in two separated figures. The other six catchments are in Fig. 5.4.

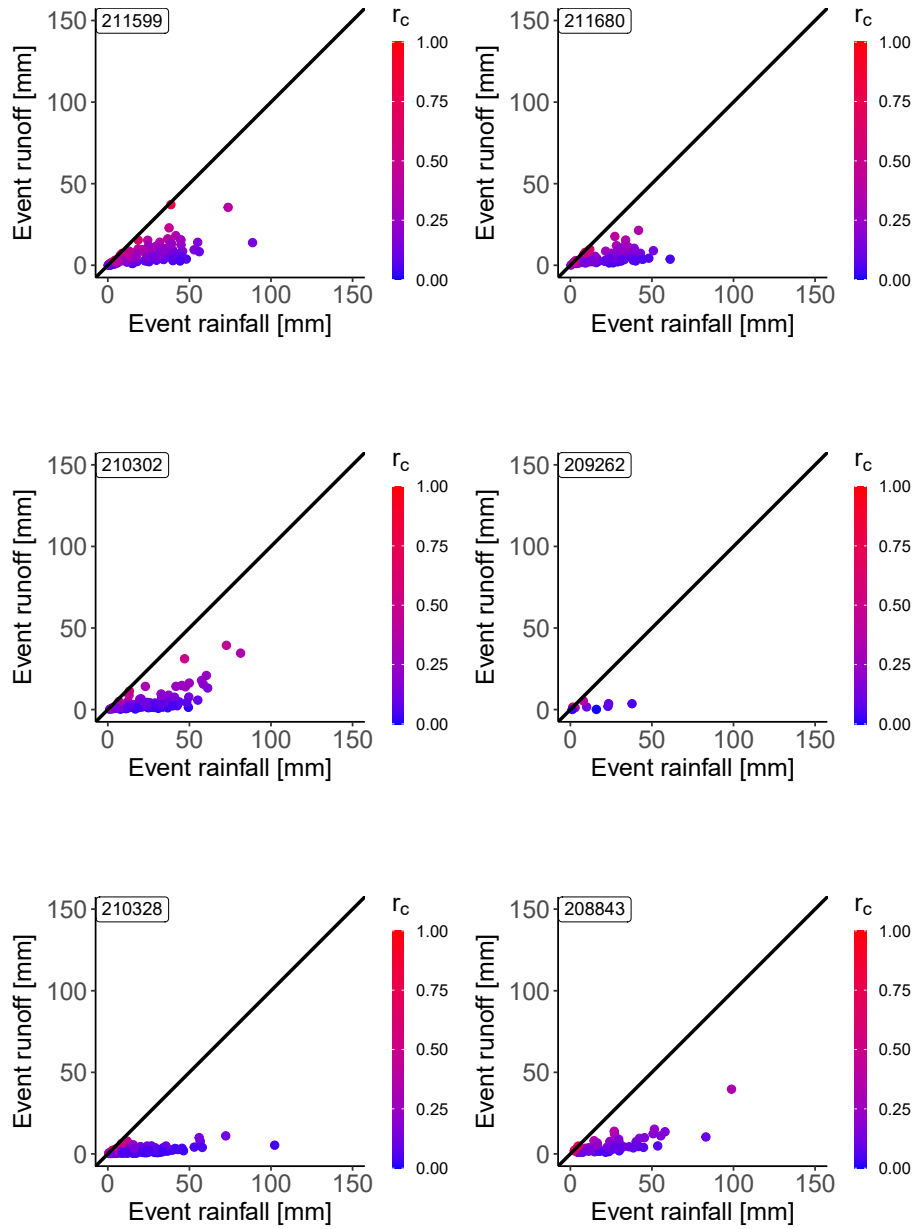


**Fig. 5.4.** Event runoff depth vs. event rainfall volume for all the catchments analysed. The plots are divided in two separated figures. The other six catchments are in Fig. 5.3.

## 5.5 Runoff coefficients distribution

The values of runoff coefficient are considered as a random variable but it is somehow controlled by the wetness of the system. Being in a dry region, the variability of the runoff coefficient tends to be high.

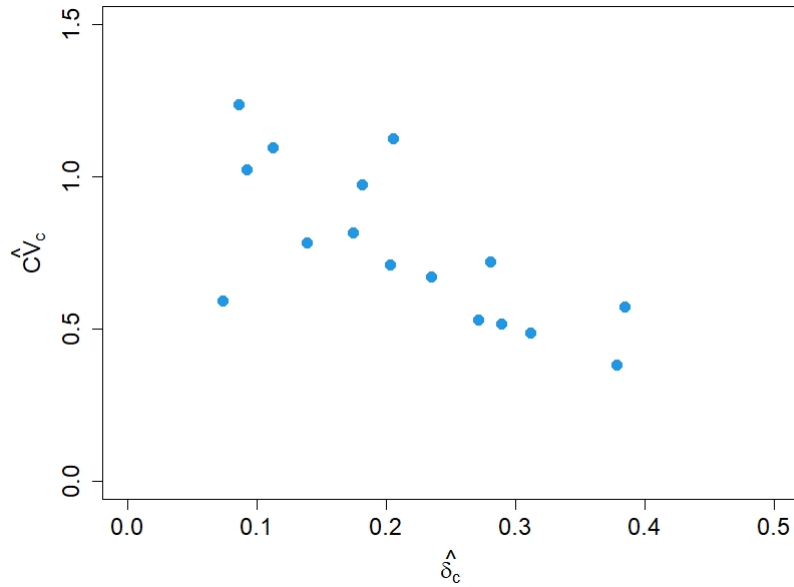


**Fig. 5.5.** Average runoff coefficient of each single catchment as a function of the variability of the events.

In Fig. 5.5 the coefficient of variation  $\widehat{CV}_c$  is plotted against the mean value of the runoff coefficient  $\hat{\delta}_c$  for each single catchment analysed. There is a decreasing trend of CV with the increasing value of the average runoff coefficient, meaning that in those catchments where the runoff coefficients are smaller, the variability of the events is much higher. On the other hand, in catchments where the average runoff coefficient is higher, CV has a lower value, meaning that the variability of the events is smaller. Here, there are not so many points (as the catchments considered are only twelve) but the results are in correspondence with the results of Merz et al. (2006), also reported in Fig. 3 of Viglione et al. (2009b).

To visualize the variability of each single event, the runoff return period is plotted against the rainfall return period in Fig. 5.6; in the Appendix B.4 there is the same plot for each single catchment individually.

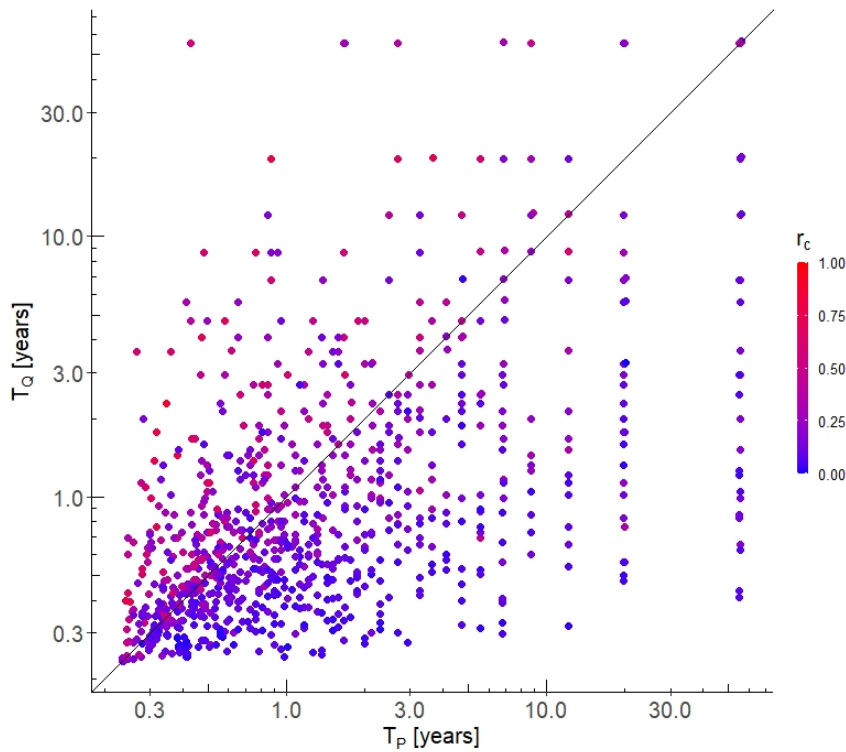


**Fig. 5.6.** Relationship between rainfall return period  $T_P$  and runoff return period  $T_Q$  for every catchment analysed. Each single point correspond to a single event and it is coloured according to its runoff coefficient. Here the rainfall return period is the one with the duration that produce the higher return period.

In this graph it can be seen the characterisation of each single event according to its runoff coefficient; in this way, to a single point is assigned the return period of the rainfall and of the runoff of the same event. The return period of the rainfall has been chosen from the plotting position method, in particular the one with the duration of the averaging time window that gives the higher return period. In this way it is possible to analyse the critical duration only.

The majority of the events are placed in the lower part of the graph being not extreme events.

Most of the events above the bisector, meaning a runoff return period higher than the one of the rainfall, have a runoff coefficient that is much higher than the mean value. This is because the catchments are in a dry region in which high flood peaks do not happen so often. In this kind of system, extreme events are not

frequent but the variability of the runoff coefficient allows to have some unusual events.

While in the right part of the graph (right with respect to the bisector) almost every events have a low value of runoff coefficient, in the left part of the graph there is not a common situation. Most of the events are generated by an higher value of runoff coefficient but some events with lower value of  $r_c$  can fall in this part of the graph. The results would be different in a wet system in which high flood peaks are more common thus, the return period of runoff are not so high and the points would be more concentrated on the right part of the graph.

What is important to notice is that the runoff return period could be much higher than the rainfall return period of the associated event. One of the reasons could be the event duration as a driving factor in the runoff generation. As explained in (Viglione & Blöschl, 2009a), if the rainfall duration is on the order of the catchment response time, it can generate an extreme flood or a flood with an higher return period.

There is also a pattern on the edge of the graph due to the Gringorten formula in which the extreme return periods are a function of the size of the data set.

## 5.6 Ratio between return periods

In the engineering practice, the target is to predict the flood peak with the same return period of the storm associated. We know that in the design storm procedure, it is necessary to choose a runoff coefficient to convert the storm event into a flood event.

As we have seen in the previous chapter, the variability of the runoff coefficient, specially in a dry region is high, leading a large range of runoff coefficients to be possible.

One of the main goal of this thesis is to try to define a value, or a range of values, of runoff coefficient to be used in the design storm procedure to retrieve the matching between the rainfall return period and the runoff return period. To do so, the ratio between the return period  $T_Q/T_P$  is analysed to try to find a pattern in the distribution of the runoff coefficient.

In Fig. 5.7 all the events with a duration (aggregation level in the IDF curve) that maximise the rainfall return period are reported, for each single catchment.

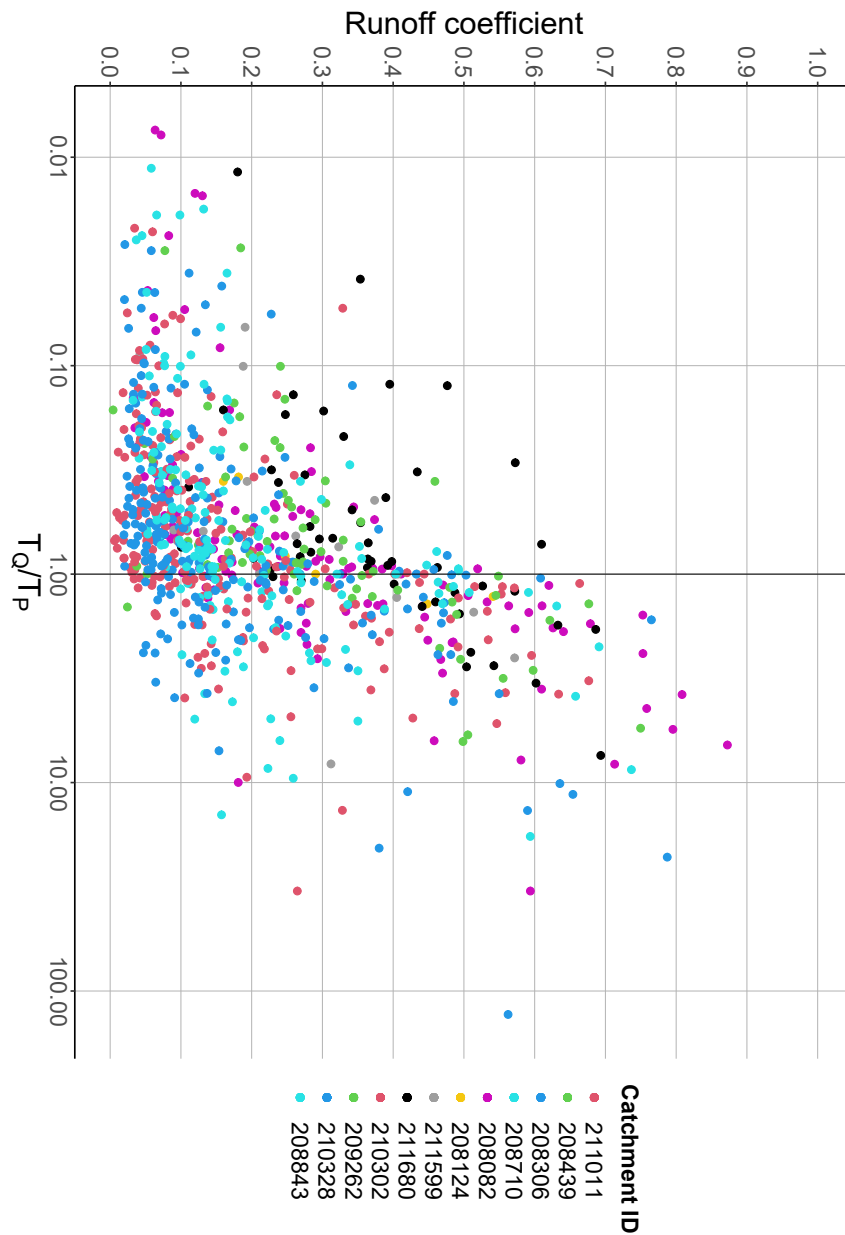
As it can be seen in the left part of the graph, events with lower runoff return period, meaning a lower  $T_Q/T_P$ , are characterised by a very low runoff coefficient. Facing events with an higher ratio between return periods, the variability of runoff coefficient starts to play an important role, in fact, there is not a clear runoff coefficient that generates events with a specific magnitude or a range of magnitude.

The majority of the flood events, even if they are very small, are generated by a precipitation that could be very extreme. Hence, the reason of the low runoff return period should be attributed to the very low runoff coefficient (left region of the Fig. 5.7). Moving to the right part of the graph, it can be seen that the return period of the quick flow could be up to 10 times the rainfall return period, in most of the case. There are also some very extreme events in which the runoff return period could be even hundred times the one of the precipitation. In the Appendix B.6 it is possible to find all the graphs of every catchment individually with the points for every aggregation level of the IDF curve.

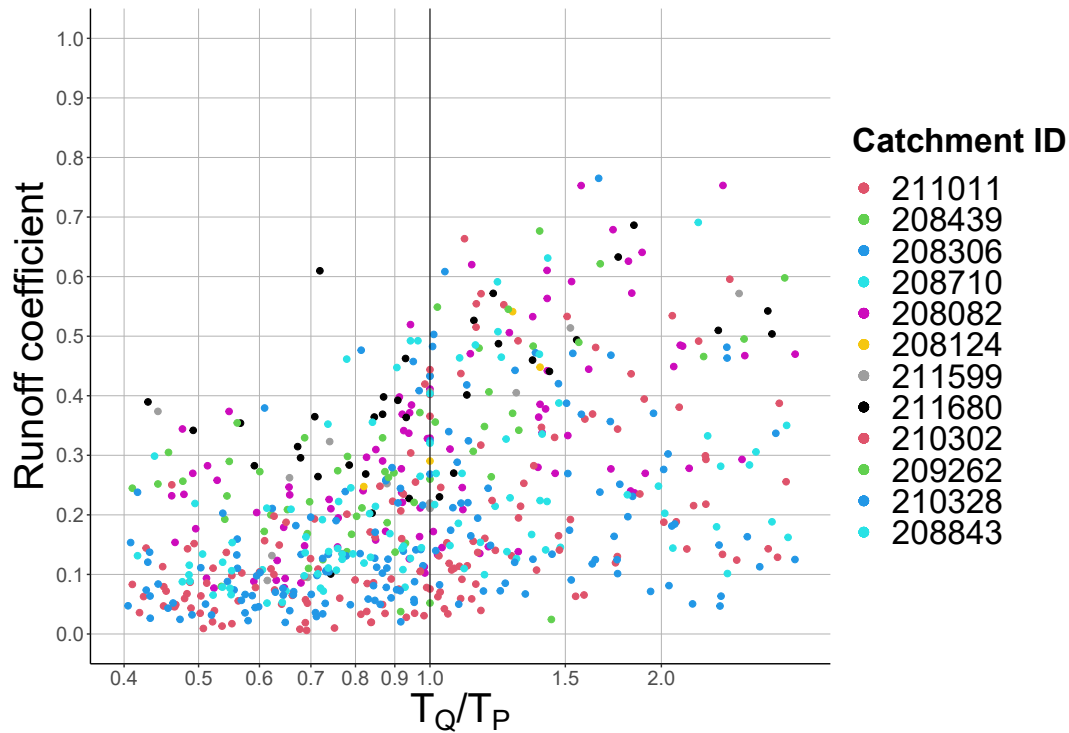
Zooming to the region in which the design storm procedure is interested, Fig. 5.8, it is possible to better understand the behaviour of the events.

Fig. 5.8 represents a slice of the previous figure, in which only the ratio of the return periods in a range from 0.4 up to 3.0 is visualized. It is difficult to choose a proper value of runoff coefficient that gives the match  $T_Q = T_P$  and there are also a lot of events with the ratio very close to one. There are few events in which the perfect matching is reached and they have a runoff coefficient that goes from a value of 0.05 up to almost 0.5 . There are also a lot of events in which the ratio is very close to one so it has been decided to treat all these events as they have the ratio equal to one.

All the points that have the ratio in the range from 0.5 to 1.5 are considered as they have that ratio equal to one in order to retrieve a distribution of runoff coefficient. It has been performed a statistical analysis because it is important to know the probability distribution of the  $r_c$ . In the next chapter the probability distribution, useful to decide which runoff coefficient needs to be selected in the design storm procedure (and its probability) is presented.



**Fig. 5.7.** Relationship between the ratio of return periods  $T_Q/T_P$  and the runoff coefficient for each catchment analysed. Each point represent a single event; the ratio between the return periods has been calculated with the maximum rainfall return period among all the "duration" in the IDF curve.



**Fig. 5.8.** Relationship between the ratio of return periods  $T_Q/T_P$  and the runoff coefficient for each catchment analysed. This figure represent a slice of the Fig. 5.7 to better understand the behaviour of the events in a region in which the engineering practice is interested.

## 5.7 Probability distribution of runoff coefficients

From Fig. 5.8 it is possible to observe that the distribution of runoff coefficient, in a symmetrical range around the ratio equal to one, can be considered similar. Starting from a ratio equal to 1.5, some events start to have a runoff coefficient higher that 0.7, this is the reason why the range were cut to a value of 1.5 .

Selecting only those events with the matching between the return periods or those events that have a ratio close to one (and all those events treated as they have a ratio close to one), it is possible to analyse the probability distribution of the runoff coefficients that generate the runoff.

In Fig. 5.9 the runoff coefficient is plotted as a function of the return period in

which the latter could be dependent from the former. There could be an increasing of the  $r_c$  with the increasing of the return period.

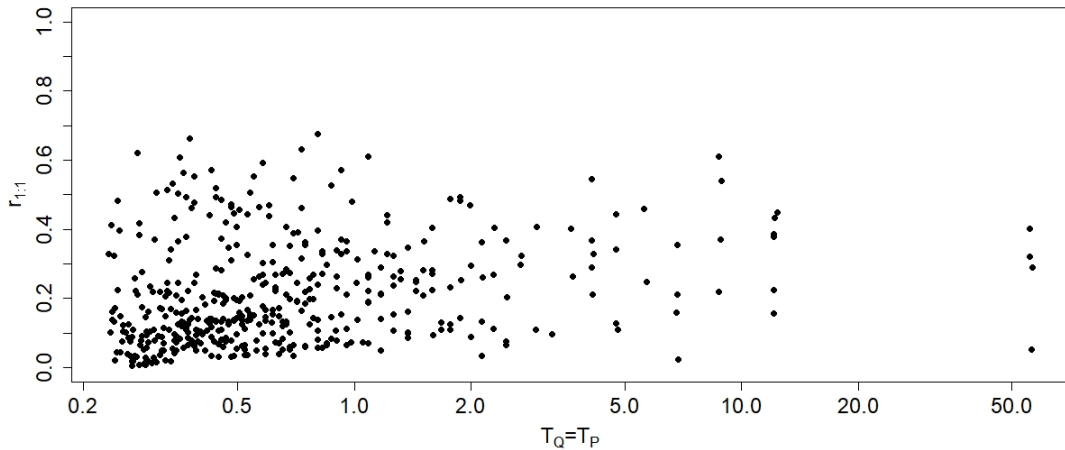


**Fig. 5.9.** Relationship between the runoff coefficient of every event, with a ratio  $T_Q = T_P$  in a range from 0.5 to 1.5, and the return period.

Again in this case, the variability of the runoff coefficient in a dry region affects the results, in fact there is not a clear distribution of  $r_c$ .

It is worth to notice that the variability of runoff coefficient seems to affect the smaller events, while the extreme events have an  $r_c$  lower than 0.4. As described before, the events here have a maximum runoff coefficient of about 0.68 while the maximum runoff coefficient recorded is 0.87. Both group of events have a mean value of 0.21 while the median value is different. Analysing all the events, the median value of  $r_c$  is 0.15 while the median value for the events with a ratio of return periods considered equal to one is 0.17.

The probability of non-exceedance of  $r_{1:1}$  is plotted in Fig. 5.10; in the Figure also the probability distribution of all  $r_c$  is plotted to make a comparison between the two distributions.

As it can be seen in Fig. 5.10b, the distribution reach the maximum around 0.6 while in Fig. 5.10a, the maximum is reached around 0.9 as explained before. Also from this graph it is possible to notice that the median value (quantile 0.5) of the two graphs are almost the same but the extreme values are different.

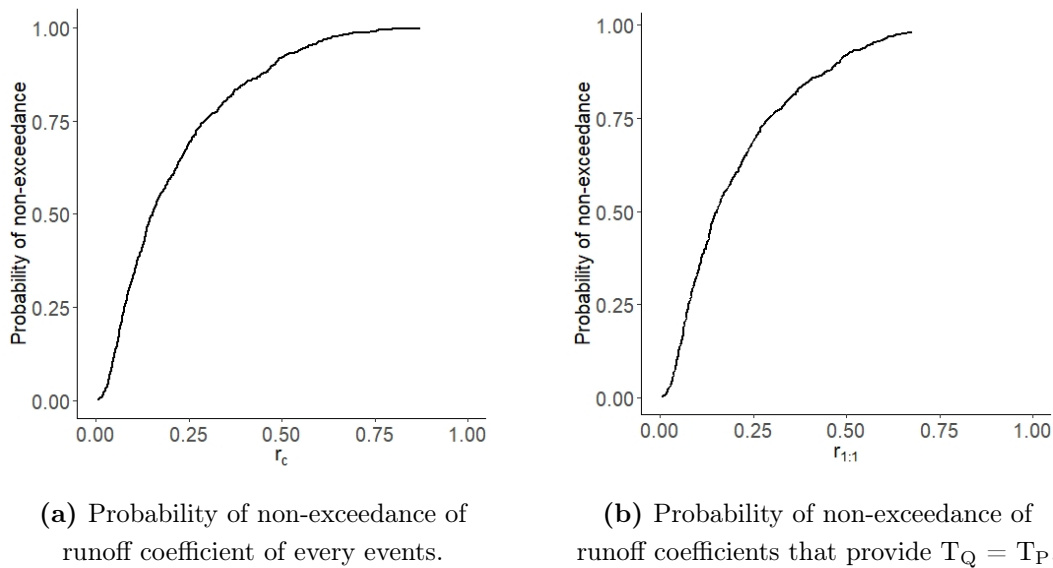


**Fig. 5.10.** Probability of non-exceedance of runoff coefficient in two different situation. The first one take into consideration every events that have been extracted while the second one considers only those event in the range of  $T_Q/T_P$  from 0.5 to 1.5 .

In the engineering practice, usually one would be interested in a probability of non-exceedance of about 80%. Looking for a runoff model in which  $T_Q$  needs to be equal to  $T_P$ , one would choose a runoff coefficient equal to 0.4, from Fig. 5.10b. This results would be different considering every events, in fact an 80% of probability would give a value around 0.3 instead of 0.4 .

The problem with the dry region is always the high variability of runoff coefficient that could be dependent from the return period.

Fig. 5.11 represents the probability distribution (probability of non-exceedance) of the runoff coefficients that give a match between the return periods, corresponding to the parent distribution (all events) and the return period associated. Each single point represents an event; only those event with  $T_Q = T_P$  are visualised and they are coloured according to the value of their runoff coefficients. Keeping out the event on the bottom right part, it is recognisable a trend going towards a probability value of about 80%. This trend seems to start when extreme events are approached; this theory needs to be confirmed looking to some very extreme

events. There is no a unique value of probability of non-exceedance of runoff coefficient that give a match between  $T_Q$  and  $T_P$  but it seems to strongly depend on the return period at the higher values. This was also confirmed by Viglione et al. (2009b) where he found a relationship between the probability, the runoff coefficient and the return period.

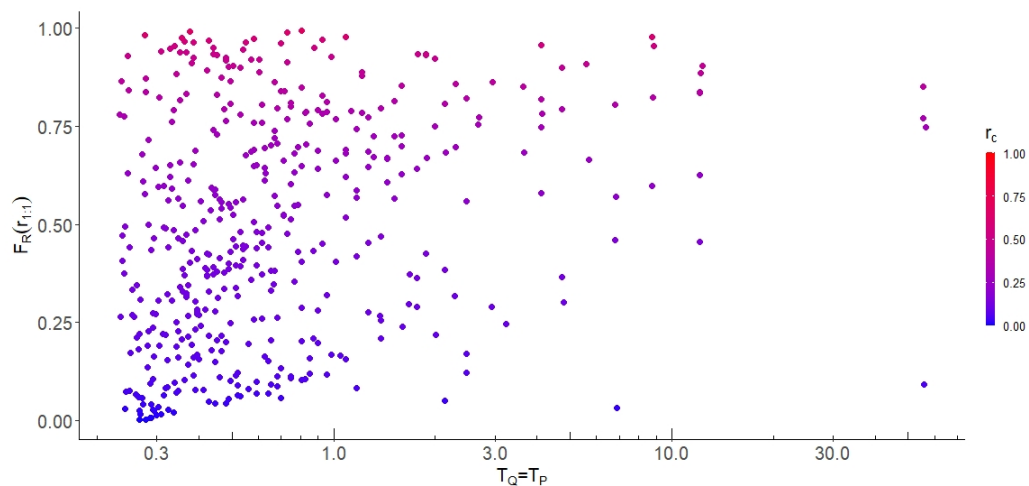


**Fig. 5.11.** Probability of non-exceedance of the event runoff coefficients  $r_{1:1}$  as a function of the return period. In this plot are reported the events in which  $T_Q=T_P$  of every catchment.

The runoff coefficients that produce the extreme events are also higher than the median value of all runoff coefficients, being the  $r_c$  of the higher return periods around 0.4 .

## 5.8 Season analysis

This chapter can be useful for some future study in order to improve the identification of a runoff coefficient that can be utilised in the engineering practice.

Taking into consideration all the events extracted within all the catchments, there are some differences among the seasons reported in the table 5.1 .

There is not a difference in the mean value while the median value of the runoff coefficient is more affected by the extreme values of runoff coefficient. In fact, considering only those event with a ratio  $T_Q/T_P$  in a range between 0.5 and 1.5 , the median value can be different.

**Tab. 5.1.** Different value of runoff coefficient based on the season analysis.

Season	N. of events	Median $r_c$	Mean $r_c$	$0.5 < T_Q/T_P < 1.5$	
				Median $r_c$	Mean $r_c$
DJF	82	0.25	0.29	0.22	0.29
MAM	185	0.17	0.22	0.17	0.21
JJA	479	0.14	0.19	0.15	0.20
SON	153	0.15	0.20	0.16	0.19

The box plots in Fig. 5.12 and Fig. 5.13 also explain this behaviour that can be attributed to the climate processes in the different seasons. The difference in the median values are not so bright but there is a sharp diversity in the extreme values that can affect the analysis. With only a few catchments and every one of them in the same region, it is difficult to see a very sharp difference; this analysis can be improved at a larger scale where the climate processes are more different.

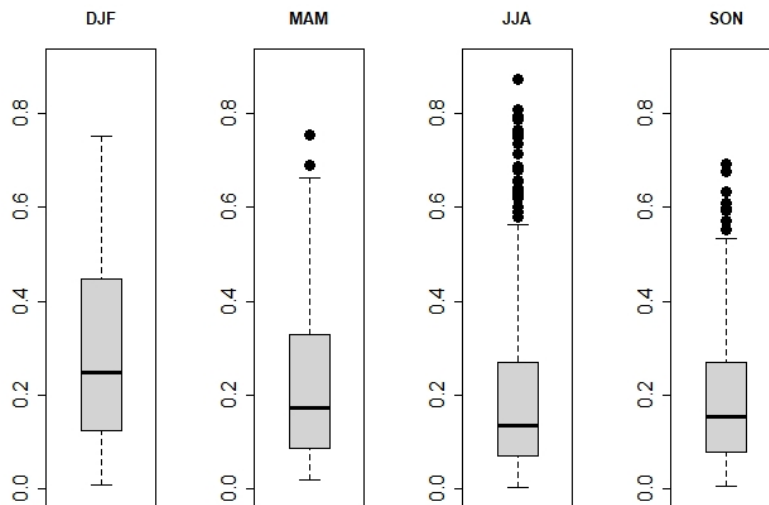


**Fig. 5.12.** Box plots of event runoff coefficient distribution according to the season. In this graph all the events extracted are considered and divided by season based on the first day of the event.

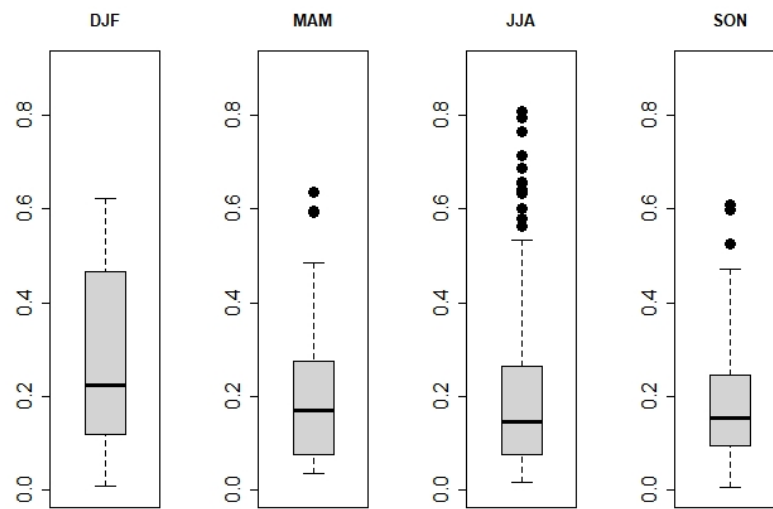


**Fig. 5.13.** Box plots of event runoff coefficient distribution according to the season. In this graph only the events with a ratio  $T_Q/T_P$  in a range between 0.5 and 1.5 are considered.

## Discussions and conclusions

The runoff coefficient ( $r_c$ ) is the percentage of rainfall that becomes direct runoff and it is easily computable as a ratio between the total volume of rainfall drained during a storm event and the amount of the precipitation of the event itself. The  $r_c$  is a fundamental parameter used in the engineering practice when it is necessary to estimate the peak flow of a flood, specially in the small to medium-size drainage basin (chapter 9.4 of Chow (1964)).

There are a lot of methods that give a guide about the procedure of the computation of runoff coefficient, when event data are not available, starting from geological information, soil cover and land use of the catchment. One of most used method is the Curve Number method from the Soil Conservation Service but, past studies have found that this method is not so appropriate for Austrian catchments. Thus, it is necessary to analyse the rainfall and runoff data trying to find, using them as a source of the real conditions, a proper runoff coefficient. The common procedure is based on the choice of the value of  $r_c$  that represents the median value of the event runoff coefficient distribution (Chow, 1964), but that choice has been debated in the literature (see e.g., Viglione et al. (2009b))

The aim of the work in this thesis is to indicate a way to select a runoff coefficient that, starting from the design storm, allows to transform the precipitation with a given return period, into a flood with the same return period. I analysed 899 events recorded at 12 stream gauges in eastern Austria and identified the ones with the return period of the rainfall similar to the return period of the runoff, which is the common assumption in the engineering practice.

The choice of the runoff coefficient, for an event with this characteristic in the region analysed in the thesis, is particularly difficult because of the large range of values assumed by the runoff coefficients, which is particularly large in the dry region of Austria investigated here (Merz et al., 2006).

The first step in my analysis is the definition of the flood events. The catch-

ments have been selected with an area ranging from 80 to 600 km<sup>2</sup>, this allows to exclude the uncertainty about the rainfall interpolation in wide territory. The region analysed is a dry region of Austria in which the solid precipitation, such as snow precipitation, is very low and it can be neglected from the runoff data recorded from the stream station. The solid precipitation can add a relevant amount of water to the runoff but it can also affect the computation of the runoff coefficient. The snow melt volume can be modelled as snow water equivalent and it can affect the runoff with a significant time delay with respect of time of precipitation. In the region analysed the snow volume is neglected so the runoff events are associated only to the rainfall event.

After the interpolation of the precipitation and the averaging within the catchment boundaries, the basin hyetograph has been extracted and it has been compared with the hydrograph of the selected stream station.

There are a lot of separation methods (Giani, Tarasova, Woods, & Rico-Ramirez, 2022) that allow the recognition of the baseflow, direct runoff and the identification of the flood events. The choice of the method is strictly subjective, thus in this thesis has been decided to use on the standard and already tested one that is the Chapman and Maxwell method. Through the event separation code, the flood events and the associated storms have been extracted for each catchment considered.

From the events extracted, my results show that in most of the case the rainfall return period is different from the flood associated. This can be explained by the different antecedent event wetness that can generate extreme flood events from very small rainfall events, on the other hand, some extreme precipitations can generate very small flood events.

In order to classify the events, a statistical analysis has been applied to the data and, using the Gringorten formula, I estimated the return period of the precipitation intensity at different concentration time and the return period of the peak flows (and they are only a function of the size of the data set).

In this thesis, the return periods are computed only from the plotting position, different results could be exploited using, for example, the Generalized Pareto distribution to extract the return period associated to the flood or precipitation quantiles.

The runoff coefficients evaluated from the rainfall events volume and from the

---

runoff events volume are screened taking only those events with a ratio  $T_Q/T_P$  in a range between 0.5 and 1.5 . Those events are considered as events with a ratio equal to one as one is usually interested in the engineering practice though the design storm method.

The variability of the runoff coefficient in the dry region of Austria is very high, as previously depicted from Merz and Blöschl (2009) and leads to equal return period events but different event runoff coefficients.

For the events analysed with a ratio between the return period of runoff and the return period of rainfall in a range from 0.5 to 1.5, the runoff coefficients assume a value from around 0.1 up to 0.7 while, considering all the events, the maximum runoff coefficient is around 0.9 .

In the design storm procedure, usually the reference value is the median value of the distribution of all observed runoff coefficients, that in this case is around 0.2 , not considering the dependence from the return period. My results show that the runoff coefficient depends on the return period of the events, specially in the extreme events.

In this thesis i considered all the events and not only the annual maxima thus, there are a lot of events with a return period lower than one year in which the variability of the runoff coefficient is large. Moving towards extreme events, there could be a stabilisation around a probability of 80 % and the  $r_c$  is around 0.4 (as also shown with the simulation method in Viglione et al. (2009b)).

This value needs to be confirmed by further studies with longer timeseries, or through regionalization methods, or with simulation of extreme events considering the variability of the precipitation which is usually assumed as a block rainfall. The simulations allow to predict events with a return period useful for the engineering practice.



# A

## Appendix 1

### A.1 Generalized Pareto code

```
#### GP TO RAINFALL ####

# number of events per year
lambda <- (length(int))/length(ys) # average number
  of events per year

# fit the Generalized Pareto to P (l-moments method)
library(nsRFA)

R_Fs<-list()
R_Pp<-list()

for (i in 1:length(Ds)){
  lmom <- Lmoments(R_D_3[[i]]$R)
  GPpars <- as.numeric(par.genpar(lmom['l1'], lmom['l2
    '], lmom['lca']))

  # RP plot
  n <- length(R_D_3[[1]]$R)
  Fs <- (1:n)/(n + 1) # non-exceedence frequency

  RPs <- exp(seq(log(0.2), log(1000), length=101))
  Fp <- 1 - 1/(lambda*RPs) # non-exceedence
  probabilities
```

```
R_Pp[[i]] <- invF.genpar(Fp, xi=GPpars[1], alfa=
  GPpars[2], k=GPpars[3]) # quantiles
}
```

## A.2 Event separation code

```
#event separation from the approach presented in merz et
al. (2006)
#eventsep.dll consists from several subrotines which are
introduced below
#####
#testing sorting routine in eventsep.dll
setwd("C:/Users/ceret/Documents/TESIVIENNA/SCRIPT/Bacini
/es")

#compiled in rtools
#gfortran -shared -o eventsep.dll eventsep.f90 sort.f90

dyn.load("C:/Users/ceret/Documents/TESIVIENNA/SCRIPT/
Bacini/es/eventsep.dll")

#read hourly discharge
#example from HOAL catchment - Xiaofei et al.2020 =
https://doi.org/10.1080/02626667.2020.1798451
tt<-read.table(paste("C:/Users/ceret/Documents/
TESIVIENNA/SCRIPT/Bacini/input_",bacino, ".txt"),
header=TRUE, sep="", row.names=NULL)

qh<-as.numeric(tt[,3])
raine<-as.numeric(tt[,4])
nh<-length(qh)

#set parameters of the procedure
```

```
parh<-c(0,0,0,0,0,0,0,0,0,0)
parh[1]=18. #khours
parh[2]=20. #kday1
parh[3]=1. #kday2
parh[4]=-900. #nodata
parh[5]=1 #iback
parh[6]=2.0 #qdrat
parh[7]=12 #imaxneigh
parh[8]=6. #tcmin
parh[9]=60. #tcmax

output<-matrix(0, nrow=nh, ncol=6)
iev<-as.integer(0)

#inputs are: hourly discharge (qh), number of timesteps
  (nh), parameters (parh)
#outputs are: number of identified events (iev),
  timeseries of baseflow. smoothed discharge, sorted
  discharge, id of events, tc of events and peak of
  events)
#all outputs are together in matrix output

dummy <- .Fortran("eventsepar", x=as.single(qh), n=as.
  integer(nh), param=as.single(parh), iev=as.integer(
  iev), output=as.single(output))

#output plotting
outp<-as.data.frame(matrix(as.numeric(dummy$output),nh
  ,6))
names(outp)<-c("Qbase", "Qsmooth", "Qsort", "EventNr", "
  Peakflag", "Tc")
iev<-dummy$iev
write.table(outp,paste("C:/Users/ceret/Documents/
  TESIVIENNA/SCRIPT/Bacini/baseflow_",bacino, ".txt",sep
```

```
    = ""))

plot(qh, type="l")
lines(outp[,1], col="red")
lines(outp[,4], col="green")

#extracting identified events
events<-matrix(NA, nrow=iev, ncol=6)

#for
for (i in 1:iev) {
  idt=i
  idstart<-min(which(outp[,4] %in% idt))
  idend<-max(which(outp[,4] %in% idt))
  events[i,1]<-idt
  events[i,2]<-idstart #start of the event
  events[i,3]<-idend
  events[i,5]<-length(which(outp[,5] %in% idt))

  peak<-qh[min(which(outp[,5] %in% idt))]
  events[i,4]<-peak
  events[i,6]<-outp[idstart,6] #tc
}

colnames(events)<-c("id", "start", "end", "peak", "
  length" ,"tc")
events

## Plotting a year to control the result
plot(qh[3500:3800], type="l")
lines(outp[3500:3800,1], col="red")
lines(outp[3500:3800,4], col="green", lwd=3)
par(new = TRUE)
```

---

```

plot(raine[3500:3800], type="h", col="blue", ylim = rev(
  range(raine)), axes=F, ylab="")
axis(4, at = seq(0, 50, by = 10))

#
#####

#event separation by using baseflow as an input -
  externally estimated baseflow can be used
#instead of a chapman digital filter used in eventsepar
  subroutine

#####
#once the events are separated, the runoff coefficient
  can be estimated
#estimation of runoff coefficients = optimised
#runoff coefficient is one of the parameter fitted to a
  simple runoff model

#using inputs = raine, qh, qbase estimated above
#model to fit

#qde=qobs - qbase
qde<-qh - as.numeric(outp$Qbase)

#simple model
runoff_sim<- function(raine, qde, param) {

  rc=param[1]
  k=param[2]
  storage=param[3]
  itevent=length(raine)
  qsim<-array(data=0., dim=itevent)

```

```
storage=0.

for( it in 1:itevent ) {

    efrain=rc*raine[it]
    qsim[it]=efrain-(efrain-storage/k)*exp(-1./k)
    storage=storage-qsim[it]+efrain

}

runoff_sim<-qsim

}

#run model with a combination of 3 parameters (rc,tc,
  storage)
pp<-c(0.3,10,0.0)

#####
#calibrate rc using automatic routine
library(DEoptim)

#objective function used in optimisation (rmse between
  observed and simulated direct runoff
rcfit<- function(raine,qde,param) {

    rc=param[1]
    k=param[2]
    storage=param[3]
    itevent=length(raine)

    rmse=0.
    ve=0.
```

```
itake=0.

storage=0.

for( it in 1:itevent ) {

    efrain=rc*raine[it]
    qsim=efrain-(efrain-storage/k)*exp(-1./k)
    storage=storage-qsim+efrain
    if(qde[it]>0.) {
        xdiff=(qsim-qde[it])
        rmse=rmse+xdiff*xdiff
        ve=ve+xdiff
        itake=itake+1.
    }
}

if (rmse>=0) {
    rmse=sqrt(rmse/itake)
    ve=ve/itake
} else {
    rmse=999.
}

return(rmse)

}

#setup of tc range used for optimization
#values 0.5 and 40 are based on original fortran code
    merz et al. (2006)

pl<-events[1,6]*0.5
pu<-events[1,6]*40.
```

```
plot(qde1,type="l")
lines(rs2, col="red")
par(new = TRUE)
plot(rain1, type="h",col="blue",ylim = rev(range(rain1*
  1.5)), axes=F, ylab="")
axis(4, at = seq(0, 50, by = 10))

#####
#script-loop to estimate runoff coefficient for all
#identified events
rain1<-list()
qde1<-list()
pl<-list()
pu<-list()
fit1<-list()
rc<-rep(NA,nrow(events))
for (i in 1:nrow(events)){
  rain1[[i]]<-raine[events[i,2]:events[i,3]]
  qde1[[i]]<-qde[events[i,2]:events[i,3]]
  pl[[i]]<-events[i,6]*0.5
  pu[[i]]<-events[i,6]*40.

  fit1[[i]] <- DEoptim(fn=rcfit, lower=c(0.0, pl[[i]],
    0.0),
    upper=c(1.0, pu[[i]], 500.0),
    control=DEoptim.control(NP=NA, itermax
      =600, reltol=1e-4, steptol=50,
      trace=10, parallelType=0),
    raine=rain1[[i]], qde=qde1[[i]])
  rc[i]<-fit1[[i]]$optim$bestmem[1]
}
```

```
output2<-cbind(events,rc)
#####unloading the dll
#unload the dll
dyn.unload("eventsep.dll")

output2<-as.data.frame(output2)
output2<-output2[order(output2$start,decreasing = FALSE)
,]
write.table(output2,paste("C:/Users/ceret/Documents/
TESIVIENNA/SCRIPT/Bacini/outputrc_",bacino,".txt",sep
=""),sep = "\t",row.names=FALSE,quote = FALSE)
```



# B

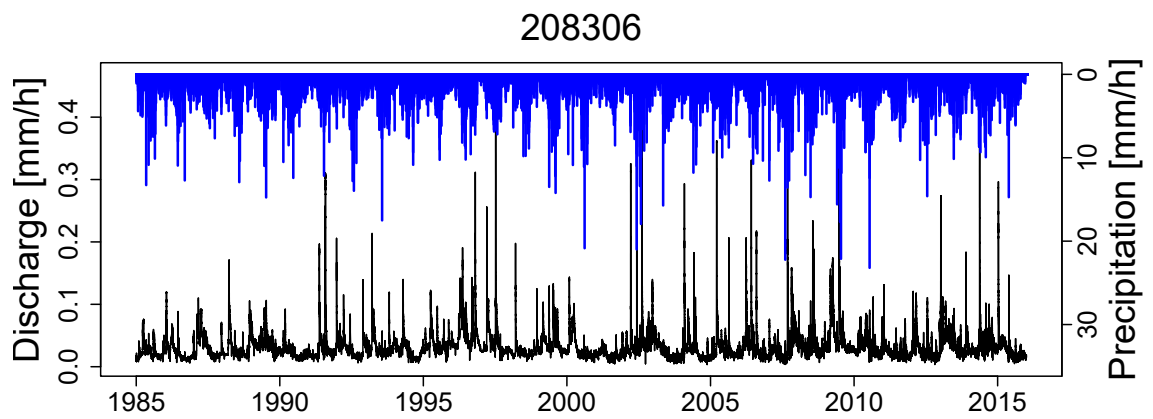
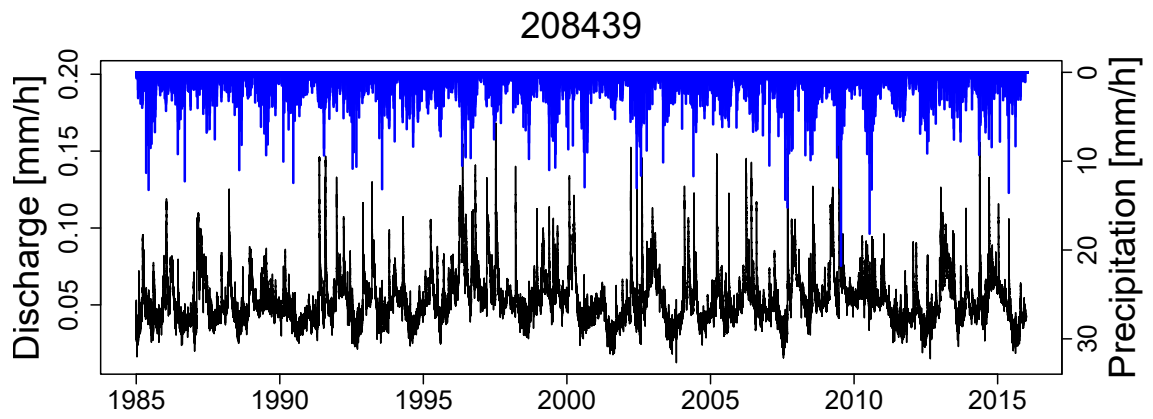
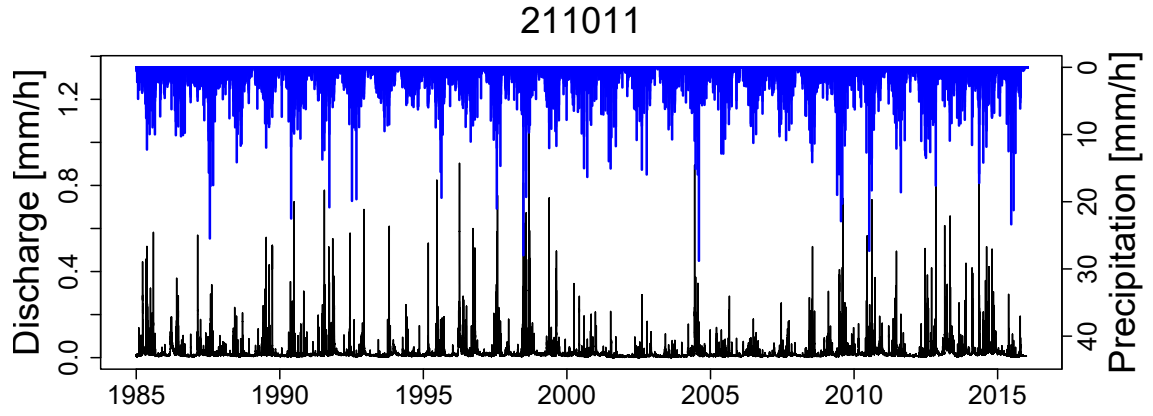
## Figures out of text

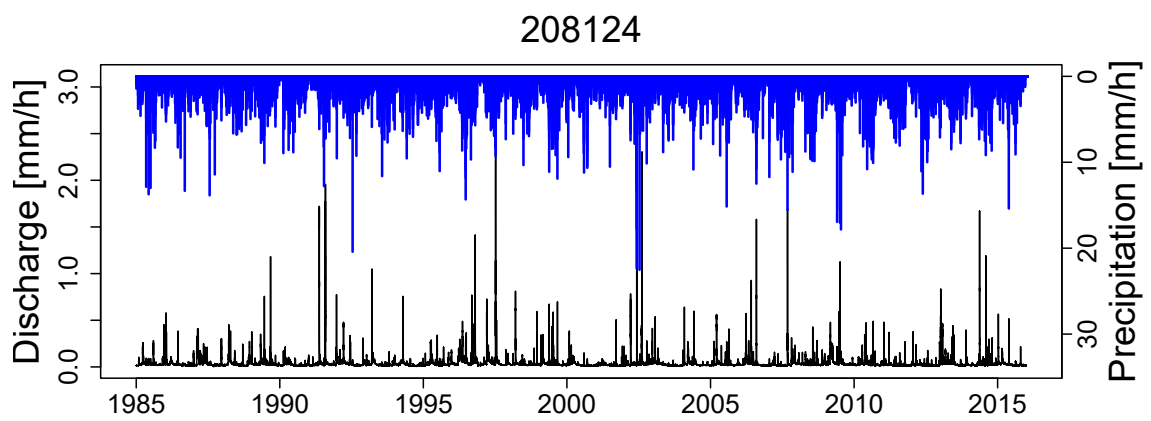
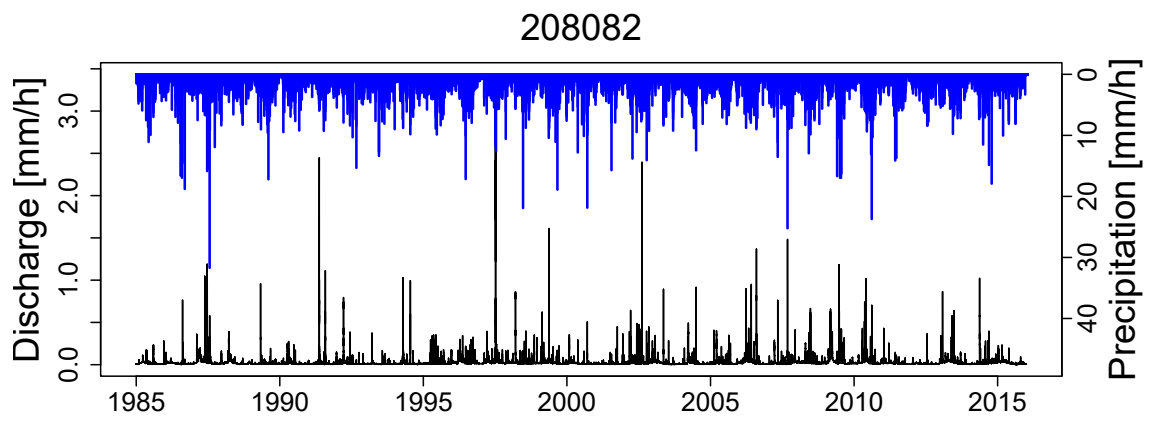
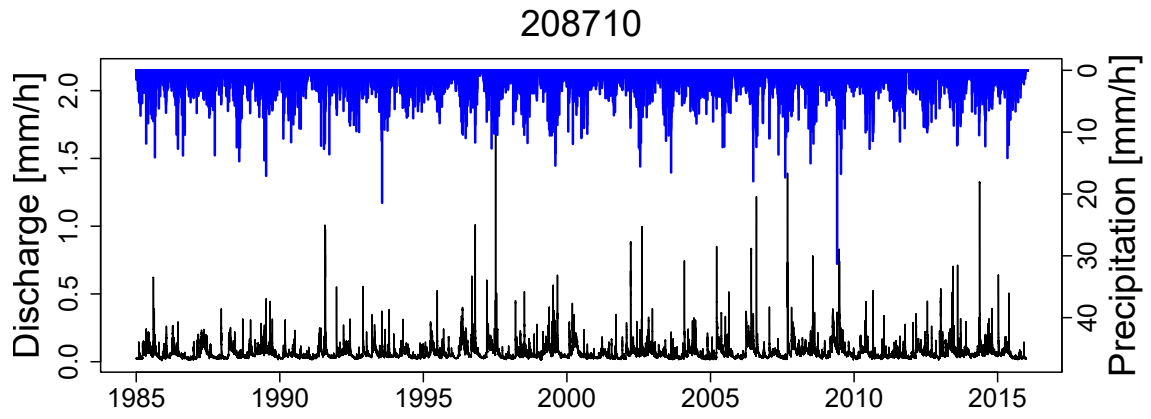
In this Appendix, all the figures out of text are reported for each single catchment separately. For simplicity, all the images will report the ID of the catchment; for this reason in the Tab. B.1 there is the information of the catchments associated to the ID.

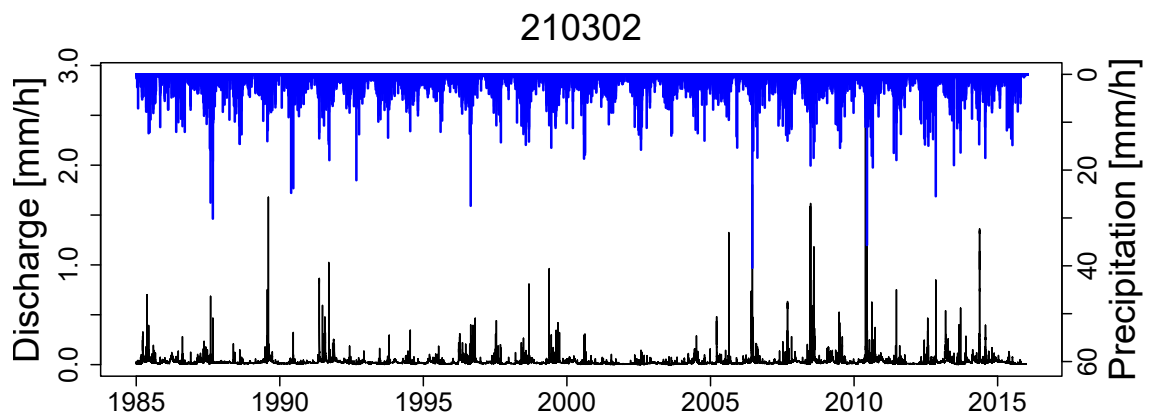
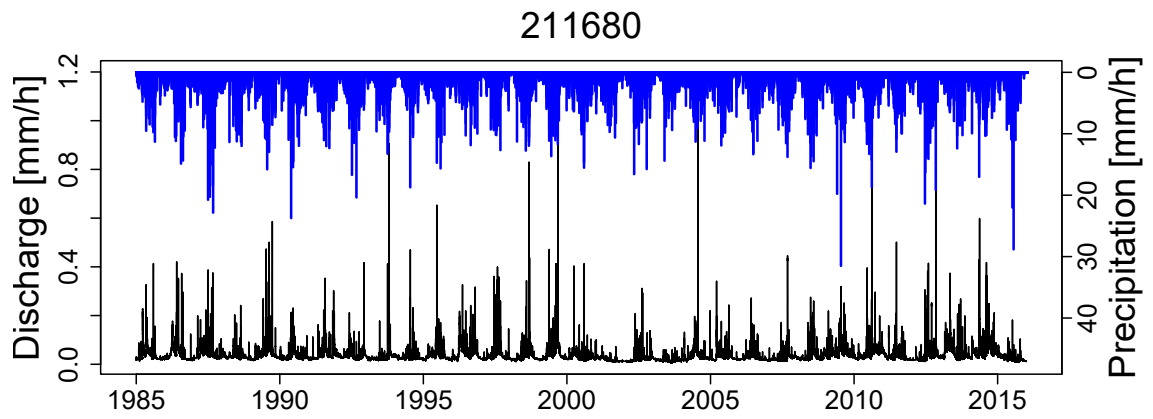
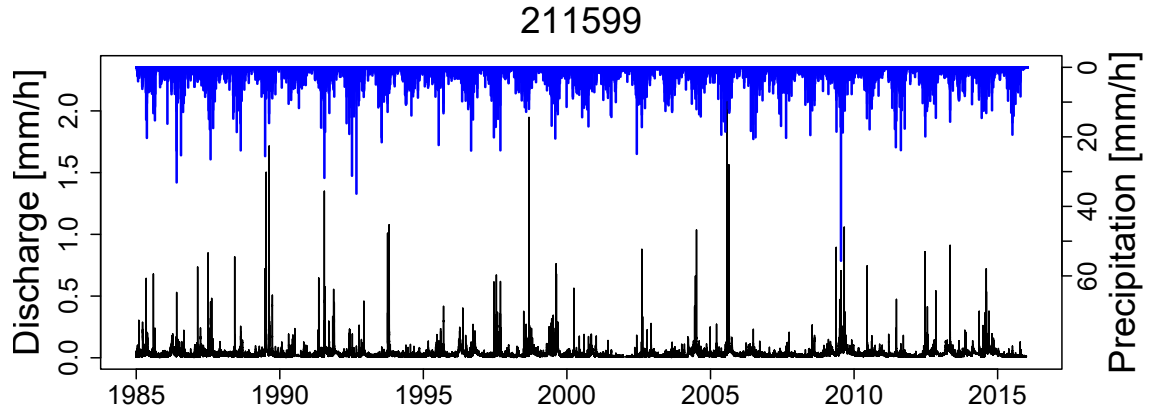
**Tab. B.1.** Information of the catchments involved in the study

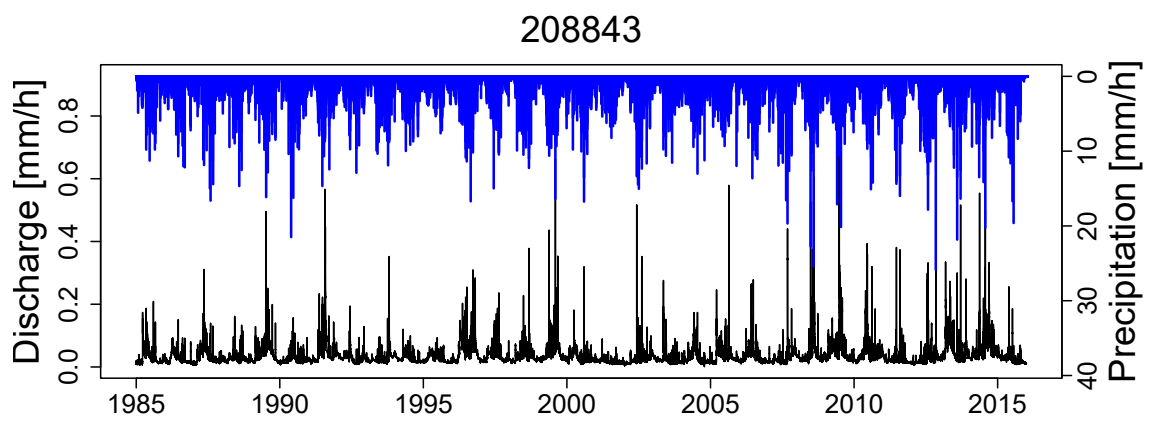
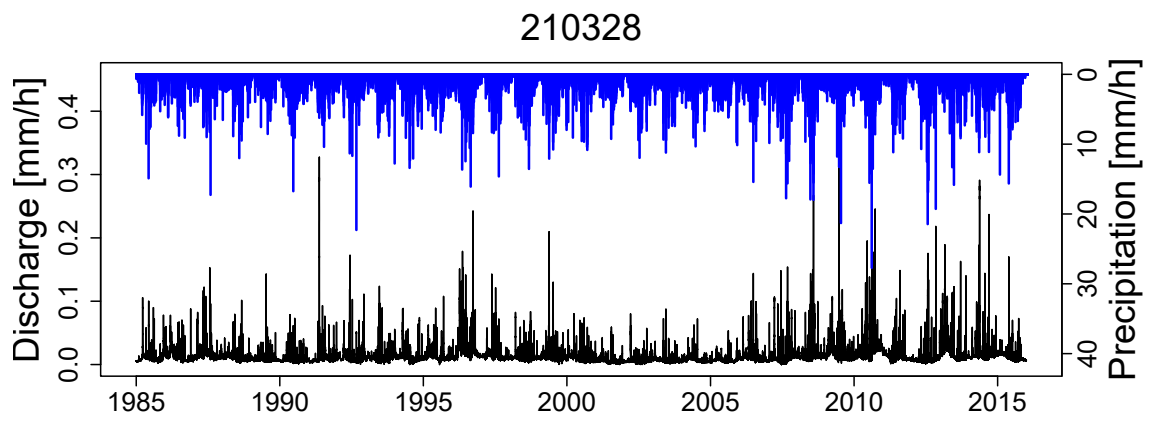
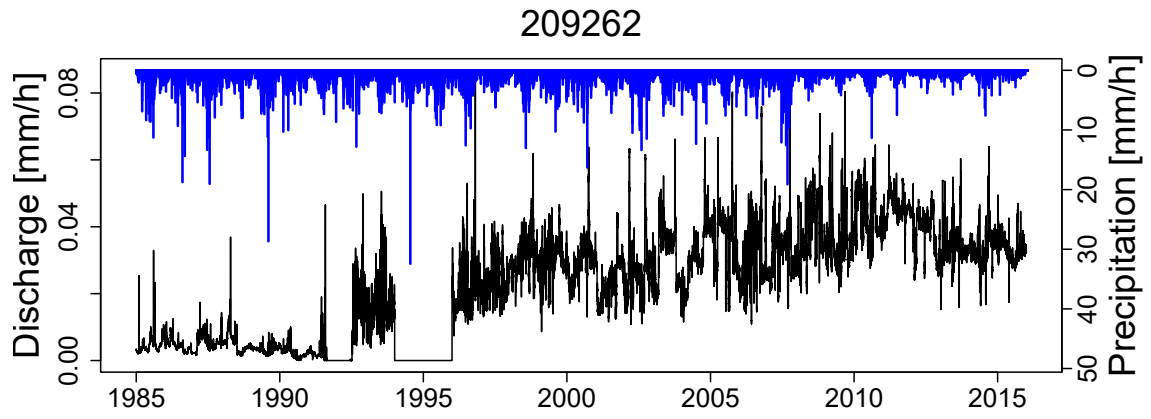
id	Stream Gauge/Stream	Elevation (m. a.s.l.)	MAP (mm/y)	Area ( $km^2$ )
211011	Waltersdorf in Oststeiermark/Safenbach	283	762.58	343.4
208439	Fischamend(Rohrbrücke)/Fischa	152	775.23	534.9
208306	Tattendorf/Piesting	221	891.46	305
208710	Gloggnitz(Adlerbrücke)/Schwarza	435	1177.27	472.2
208082	Kennedybrücke/Wien	183	747.89	199.4
208124	Hirtenberg/Triesting	277	856.99	287.3
211599	Mitterdorf an der Raab/Raab	398	940.22	183.7
211680	Hammerkastell/Lafnitz	365	916.82	285.5
210302	Kirchschlag in der Buckligen Welt/Zubernbach	408	849.29	113.6
209262	Engelhartstetten/Rußbach	138	476.45	497.8
210328	Trausdorf an der Wulka/Wulka	143	700.67	235.9
208843	Erlach/Pitten	307	887.72	412.9

## **B.1 Starting data set**

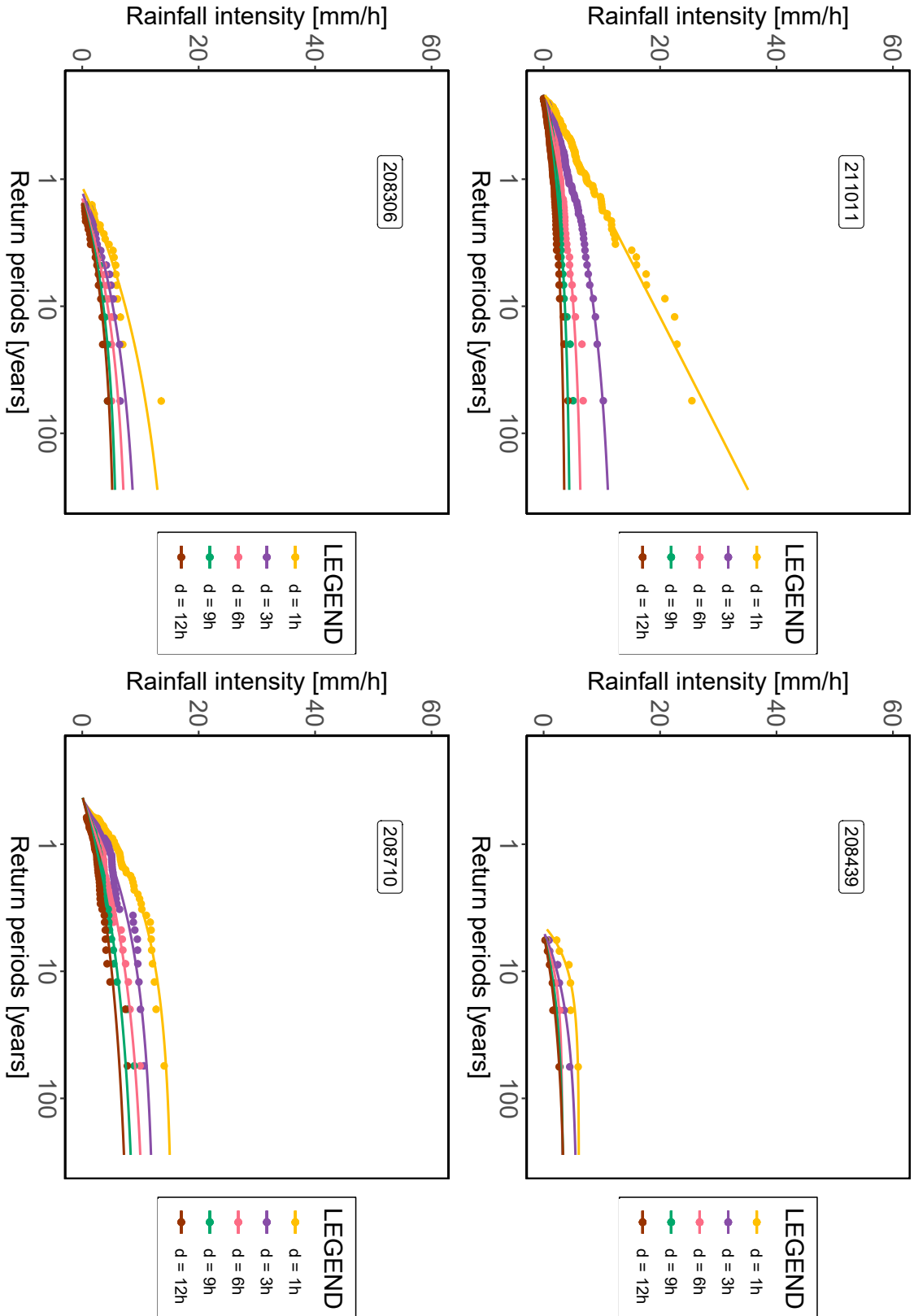


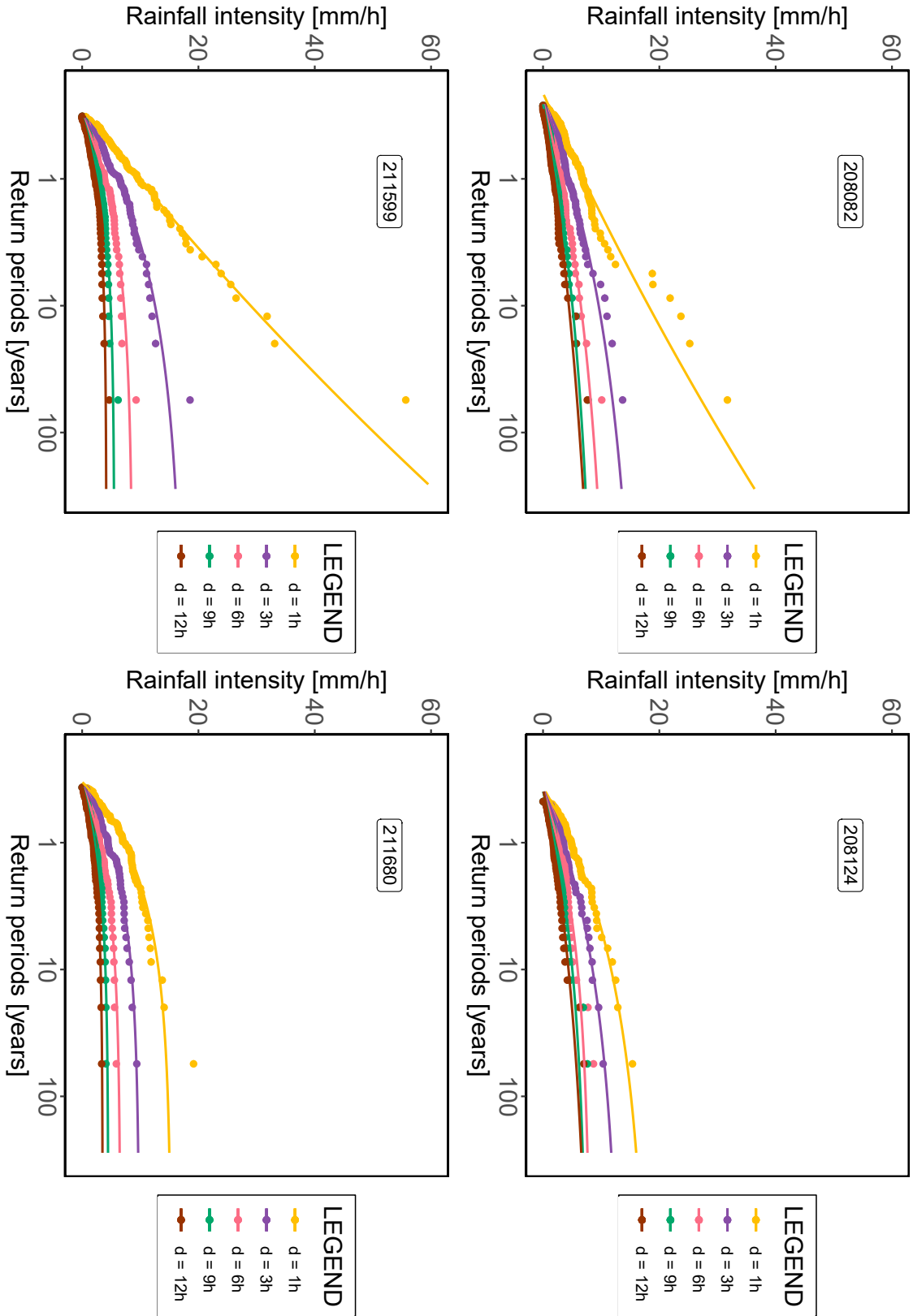


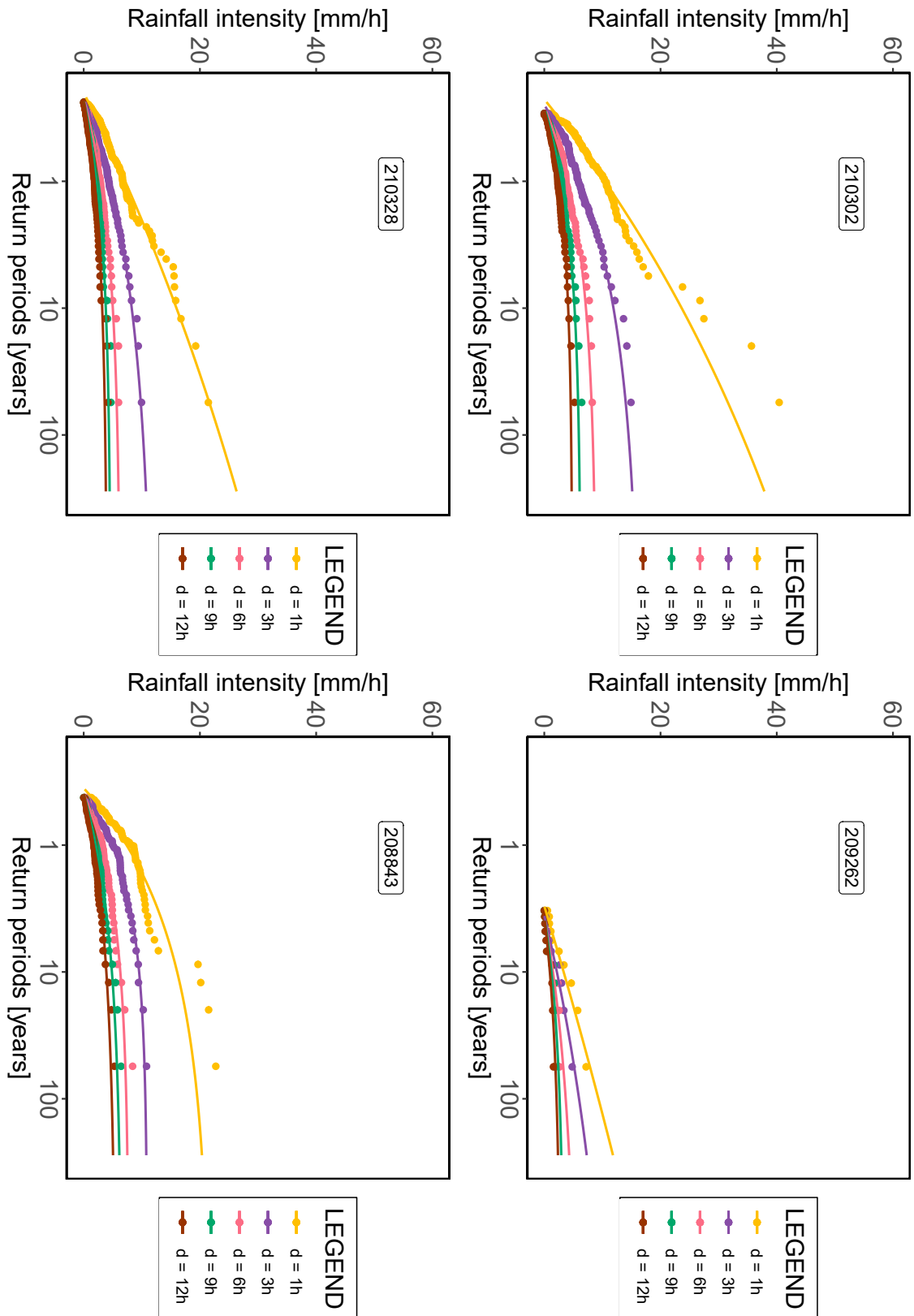




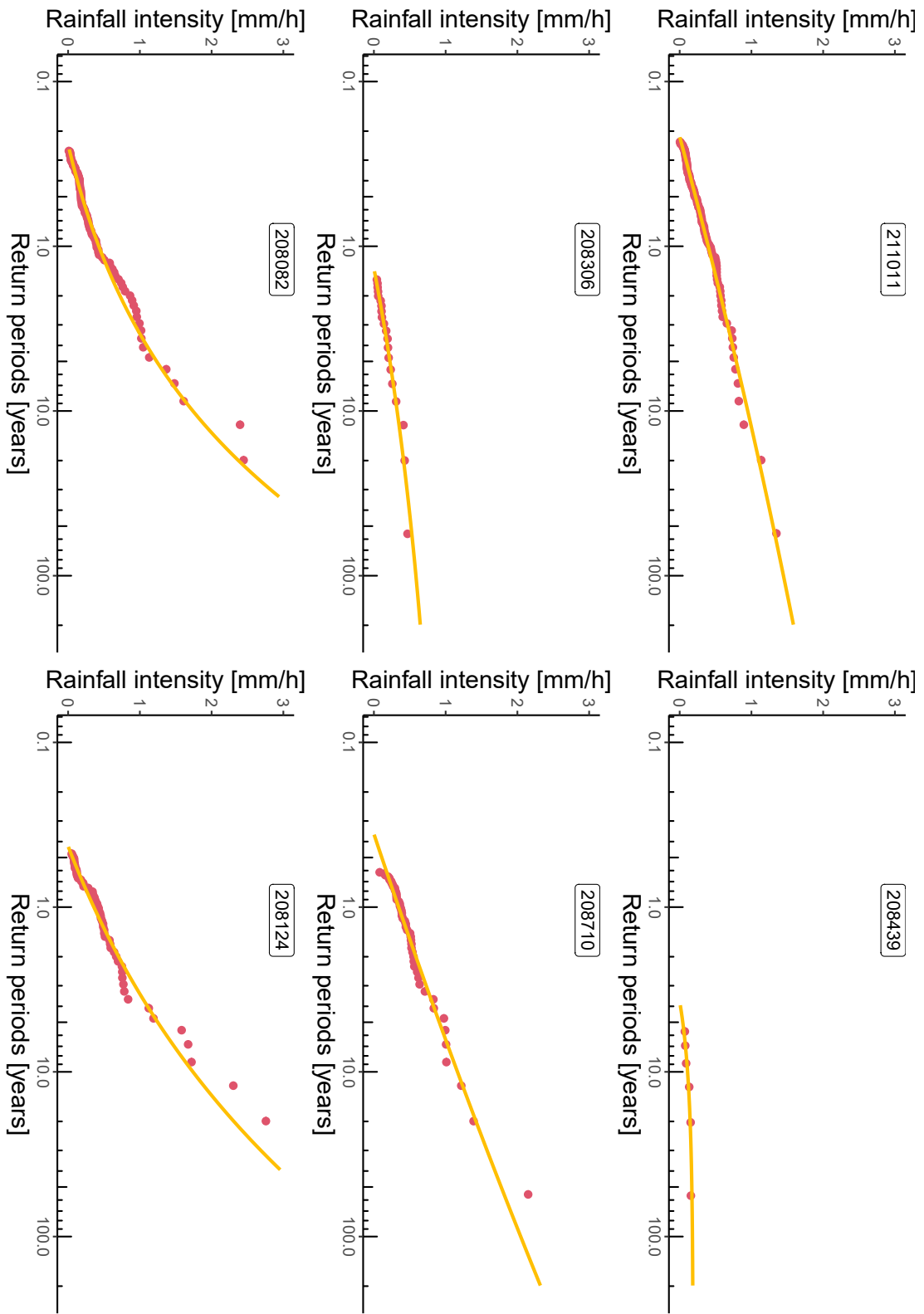
## **B.2 IDF curves**

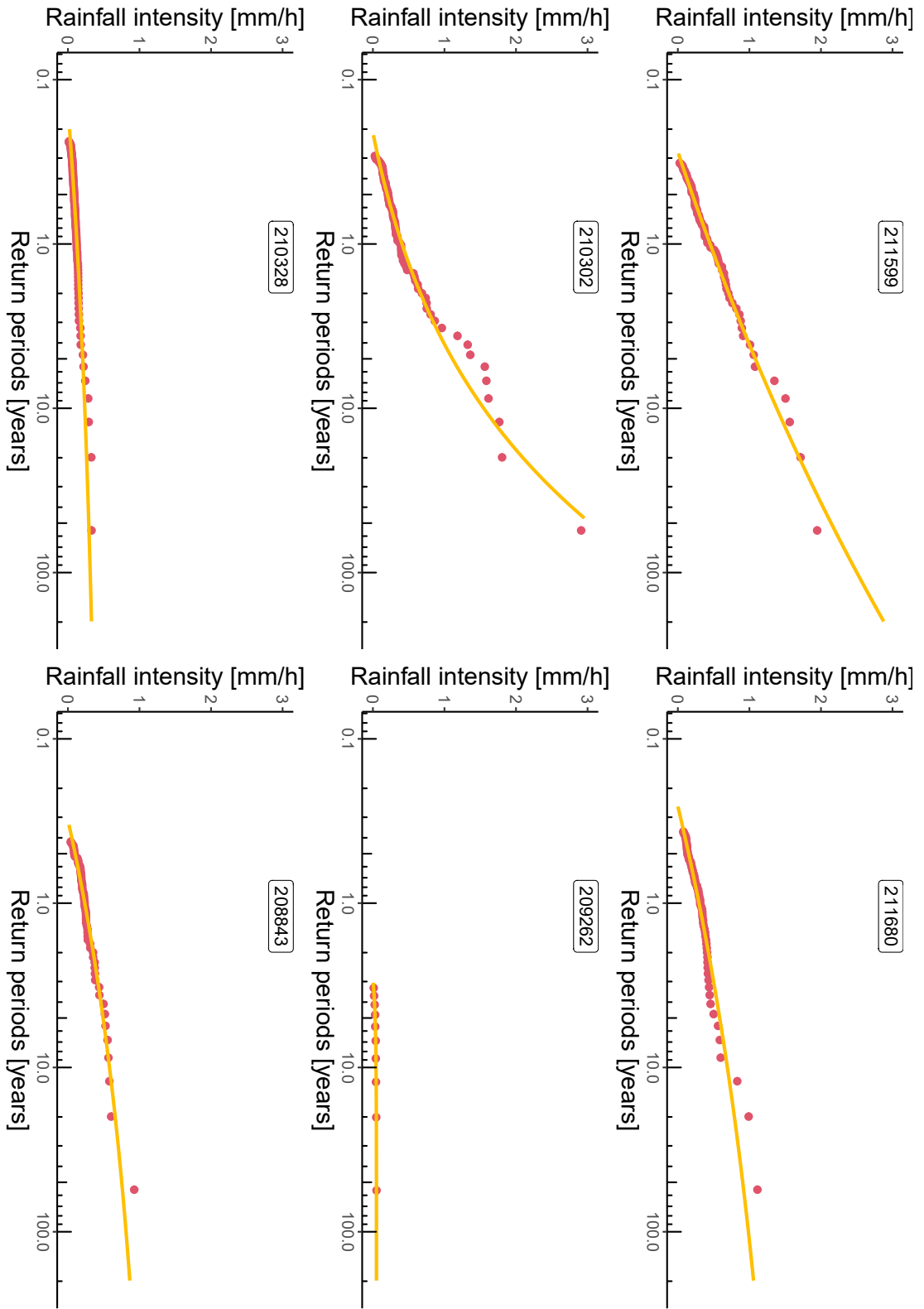






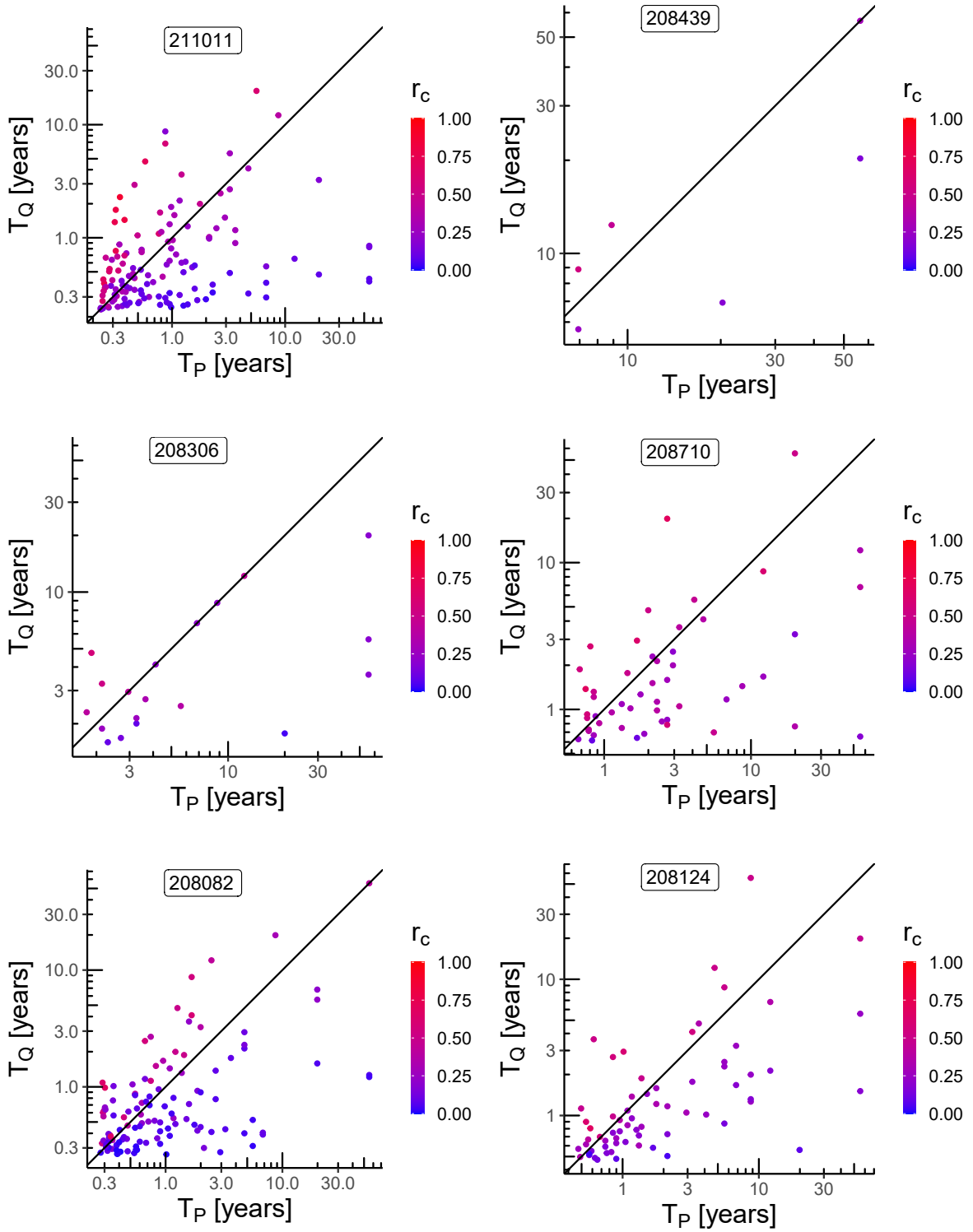
## **B.3 QDF curves**

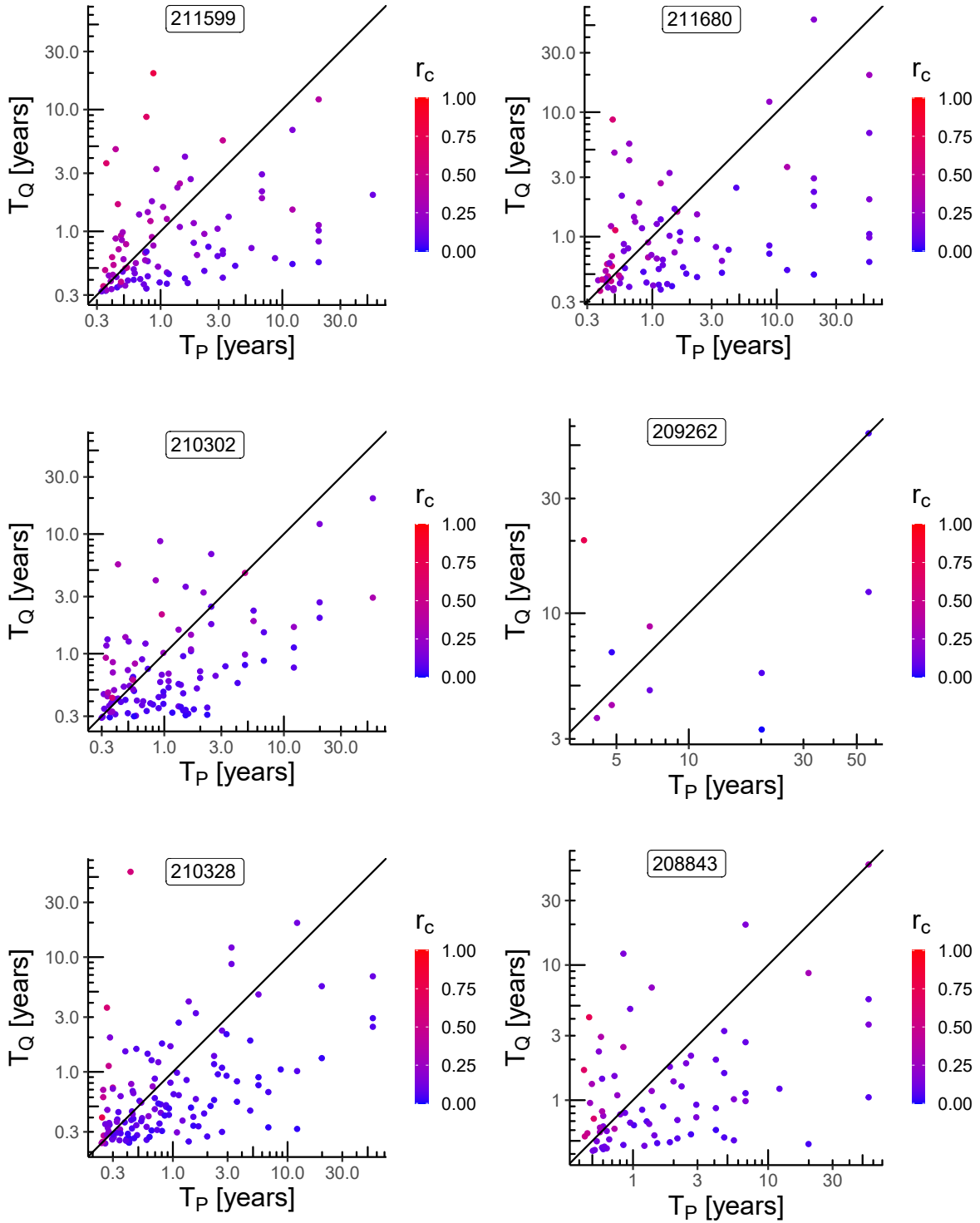




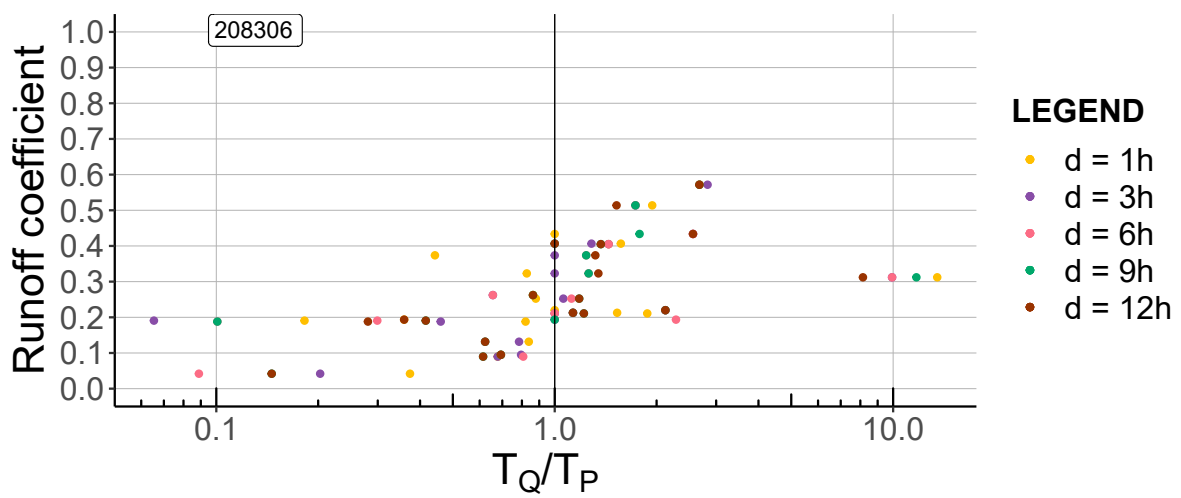
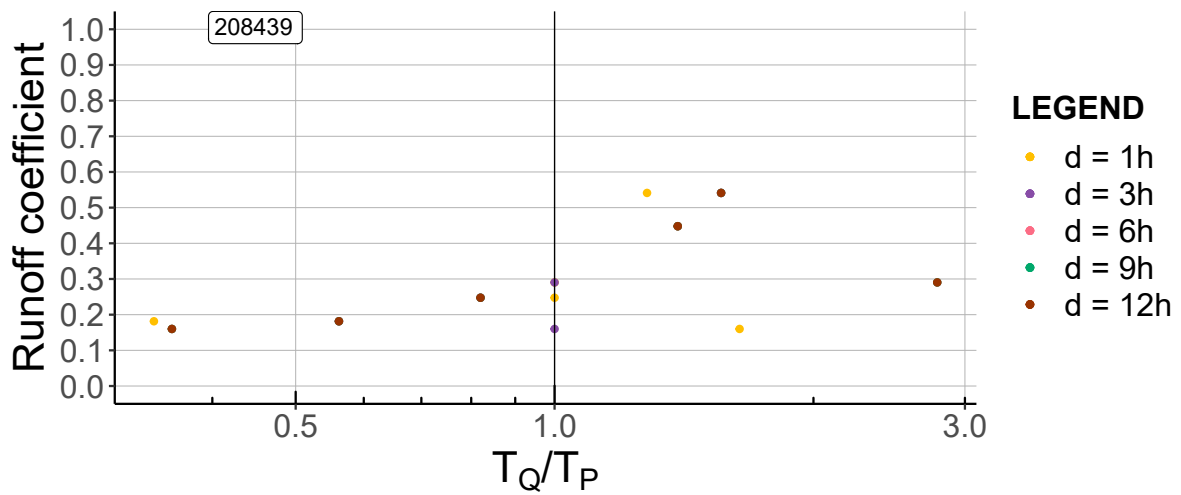
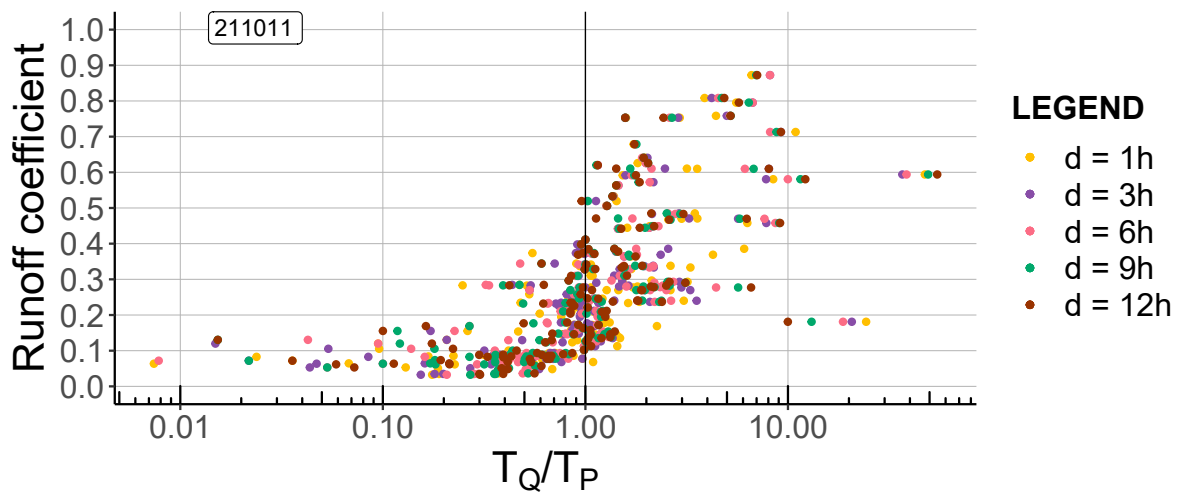
## **B.4 Comparison between return periods**

B.4. Comparison between return periods

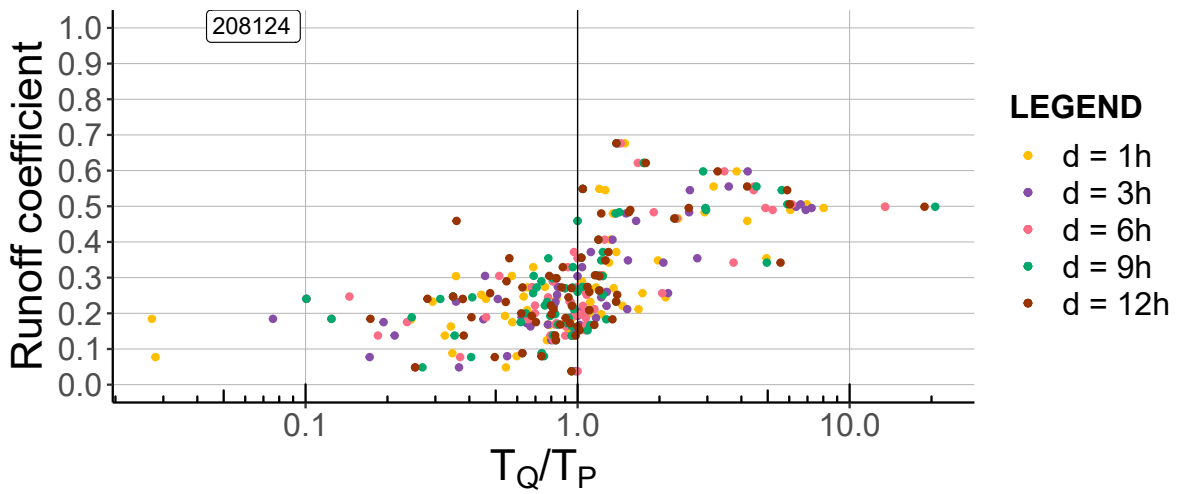
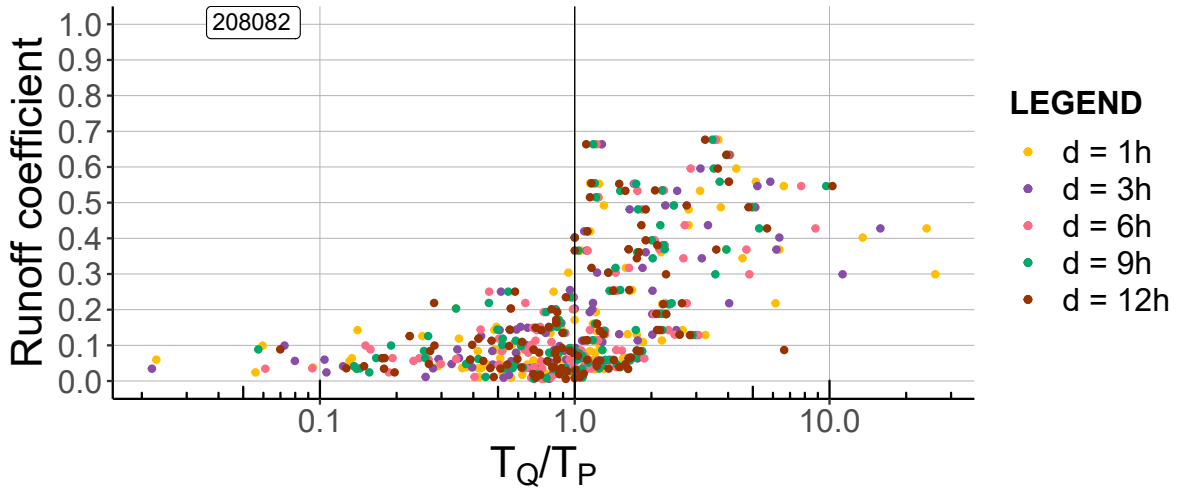
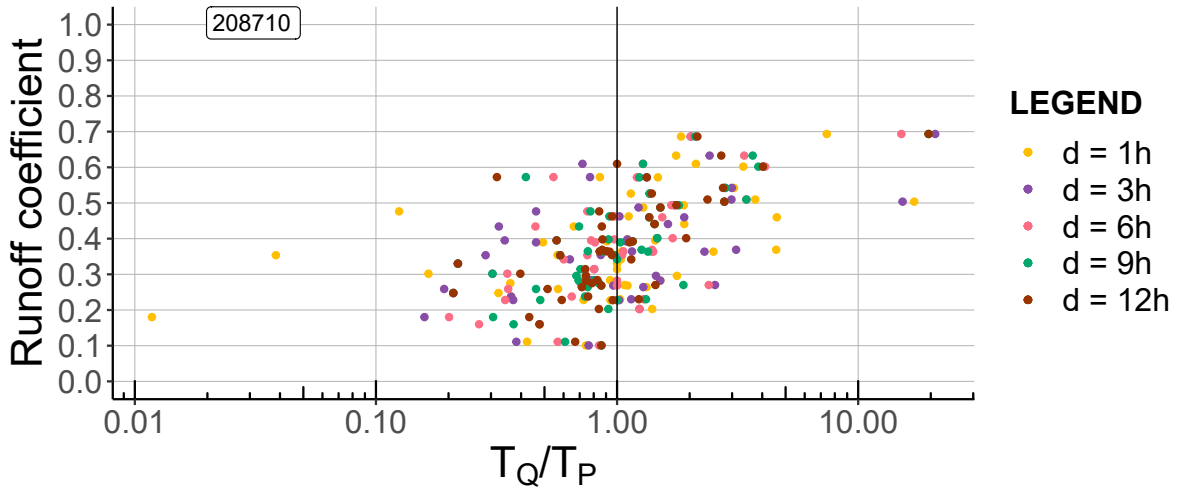


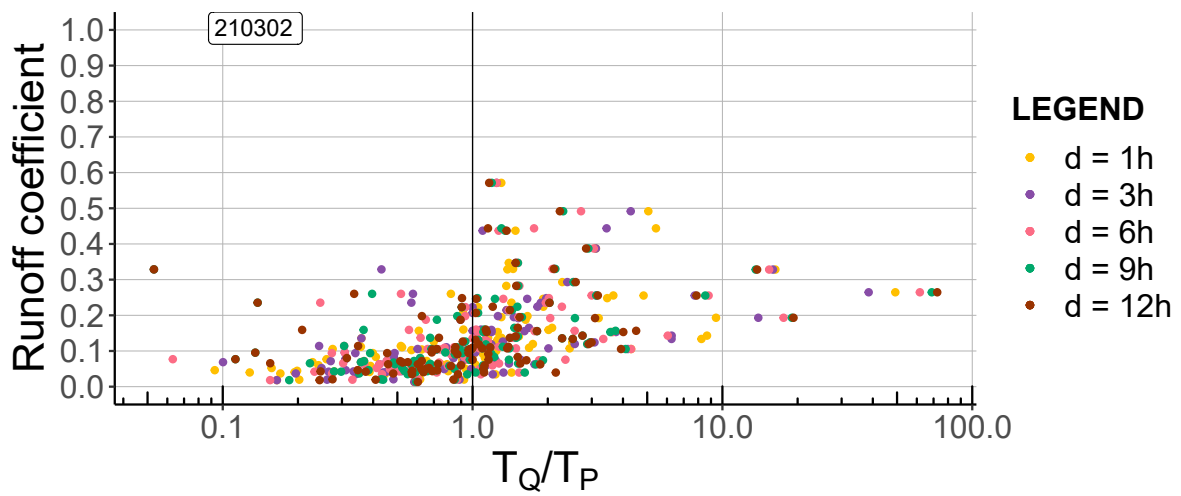
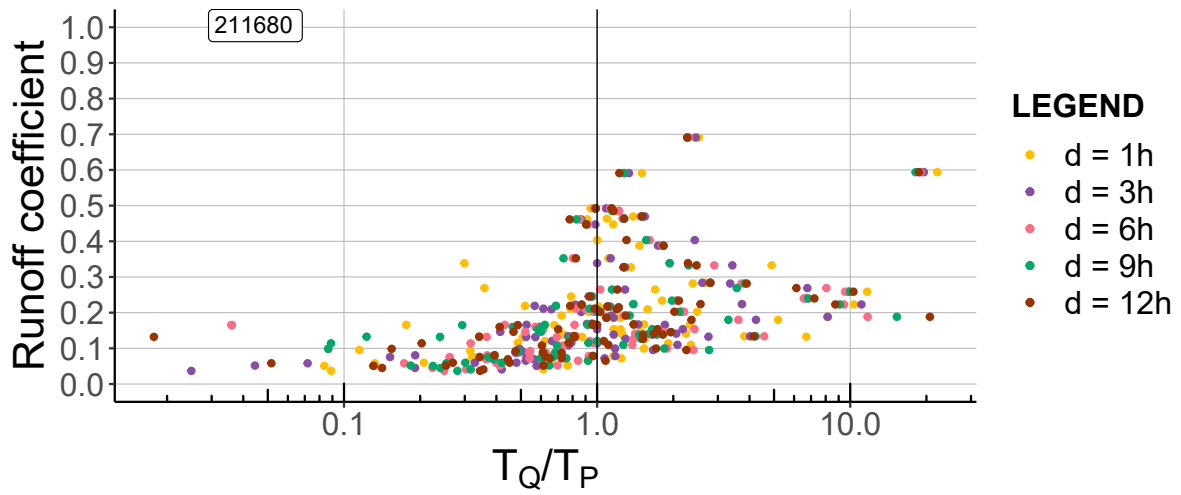
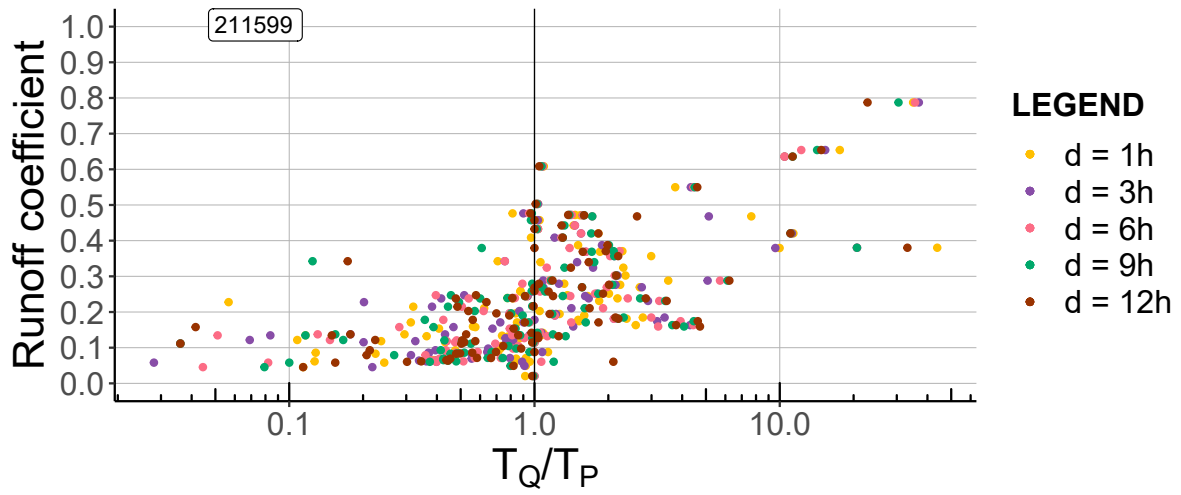


## **B.5 Ratio between return periods**

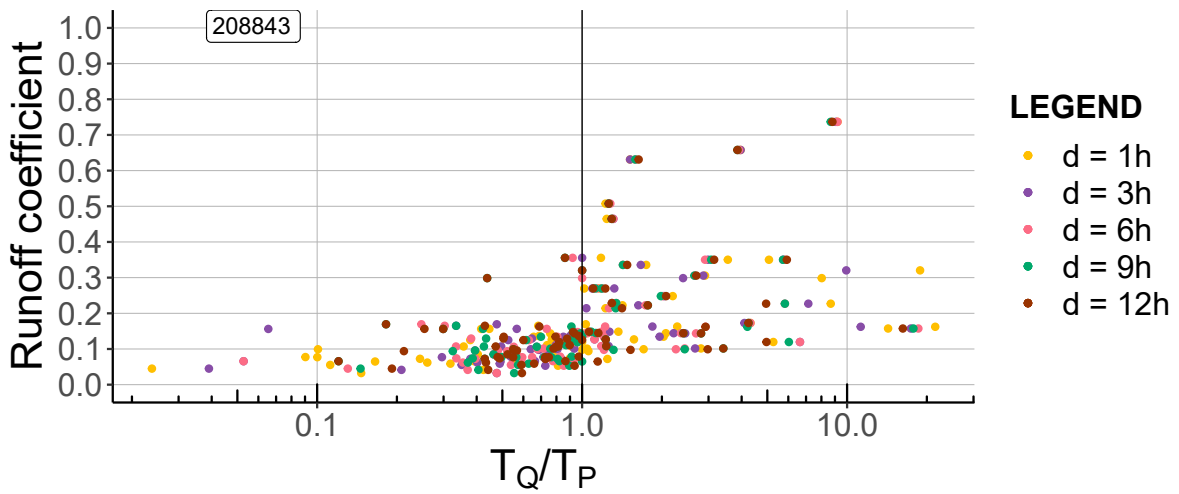
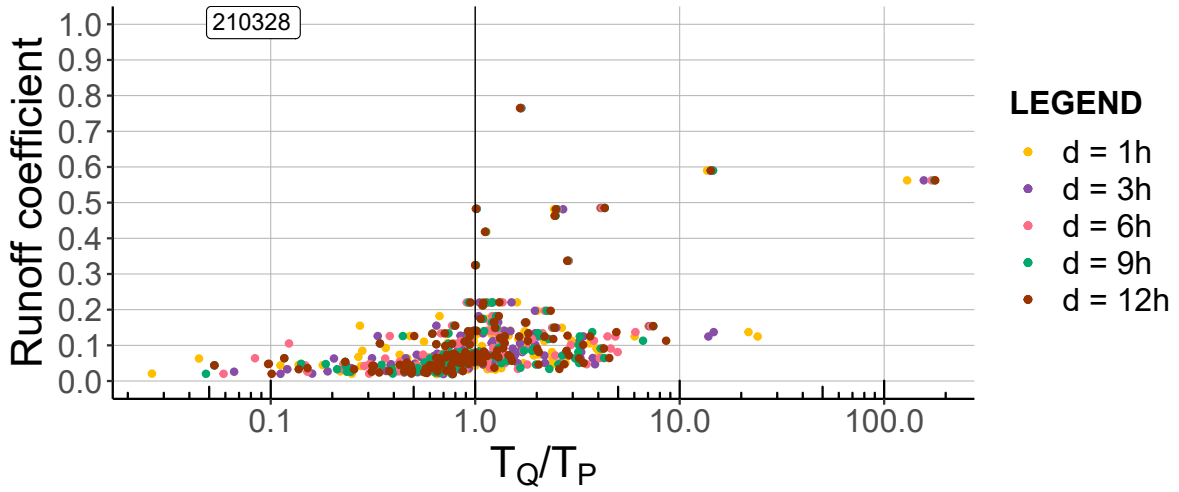
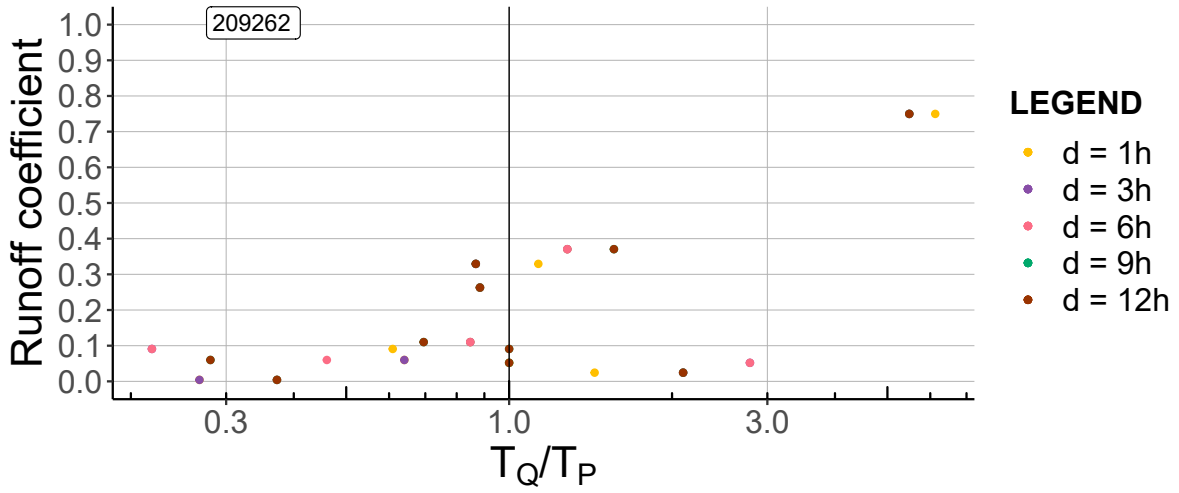


B.5. Ratio between return periods





B.5. Ratio between return periods



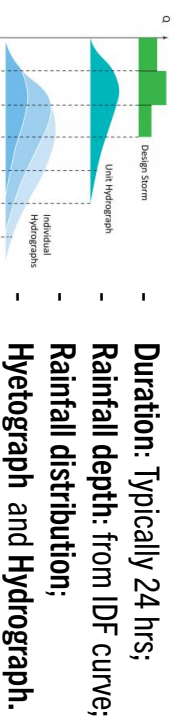
## **B.6 HydroCarpath conference**



## THE RUNOFF COEFFICIENT FOR A T-YEAR DESIGN FLOOD, USING DATA FROM AUSTRIAN CATCHMENTS.

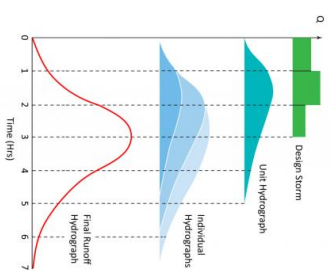


### Design storm general procedure

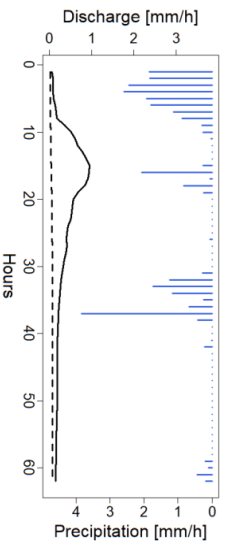


### Background Austrian knowledge

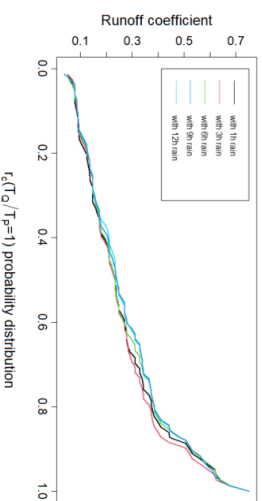
- Simplified world;
- Rainfall data set;
- Simulation of runoff;
- Hydrograph: obtained with a simulation of runoff coefficient.



## Current study



Rainfall and runoff data set  
Event analysis





## The runoff coefficient for a T-year design flood, using data from Austrian catchments



Lorenzo CERETTI<sup>1,2</sup>, Günter BLÖSCHL<sup>2</sup>, Alberto VIGLIONE<sup>1</sup>, Juraj PARAJKA<sup>2</sup>, Miriam BERTOLA<sup>2</sup>, Peter VALENT<sup>2</sup>

<sup>1</sup> Department of Environment, Land and Infrastructure Engineering (DIAT), Polytechnic University of Turin, Turin, Italy  
<sup>2</sup> Institute of Hydraulic Engineering and Water Resources Management, TU Wien, Wien, Austria

### INTRODUCTION

The **runoff coefficient** considers the amount of rainfall that becomes direct runoff and it is back calculated from the volume of rainfall fallen in the watershed considered and the volume of direct runoff measured in a river station during an event. The aim of this study is to analyze the correlation between the event runoff coefficient and catchment characteristics, with respect to the return period of the storm and of the flood peaks. The **final goal** is to detect a value of the **runoff coefficient** that gives the **discharge return period equal to the rainfall return period** which is typically assumed in the design storm procedure.

### DATA COLLECTION

- The study is set in East Austria using data from 1985 to 2015 (Fig. 1).
- **Hourly rainfall data**, from rain gauges, were spatially interpolated with the inverse distance-weighted method and then combined with the catchment boundaries to estimate **hourly catchment precipitation**.
  - Fifteen minutes discharge data were aggregated to obtain **hourly discharge data**.
  - **Baseflow separation** and **event separation** were performed to separate each event (Fig. 2).

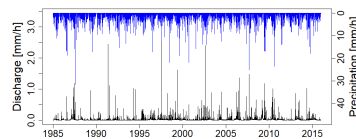


Fig. 1 Time series of runoff and precipitation for a single catchment.

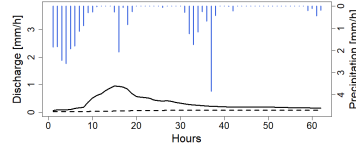


Fig. 2 Example of an identified event. The dotted line represents the baseflow and the solid line represents the runoff.

### METHODOLOGY

The design storm procedure idea is to estimate a flood associated with a return period from intensity-duration-frequency curves (Fig. 3) for the site of interest. In order to avoid underestimation of the flood magnitude, it is important to perform the frequency analysis for each catchment obtaining a return period for each intensity and duration. Then, the hydrological procedure consists in the transformation of the designed storm to a flood hydrograph with an event-based runoff model that needs to be calibrated for the catchment of interest. **Definition of the runoff coefficient** as a parameter of the model, in this type of process, is **fundamental** because **runoff is affected** by many factors that are different for each catchment.

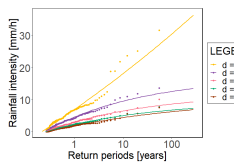


Fig. 3 IDF curve by fitting a Generalized Pareto distribution to the event rainfall data.

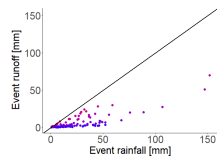


Fig. 4 Event runoff depth vs. event rainfall. The low runoff volume highlight the dry region of the catchment.

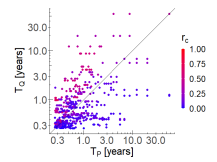


Fig. 5 Discharge return period vs. rainfall return period, coloured by event runoff coefficient.

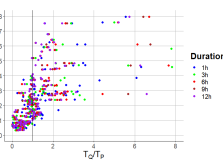


Fig. 6 Runoff coefficient vs. ratio between runoff and rainfall return period.

### RESULTS and CONCLUSIONS

The runoff distribution for the events in which TQ is equal to TP, Fig. 7, shows the probability of matching TQ and TP for each value of the event runoff coefficient.

It is also possible to evaluate the overall probability that the runoff coefficient selected in the previous graph has, Fig. 8.

Correlation between catchment characteristics and runoff coefficient distribution might explain the behaviour of the runoff events and lead to evaluate runoff coefficient in ungauged catchment in Austria.

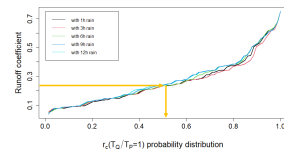


Fig. 7 Runoff coefficient probability distribution for events with  $0.5 < T_r/T_p < 2$ . This events are considered with  $T_r/T_p = 1$ .

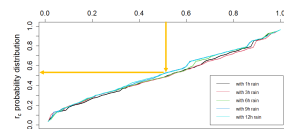


Fig. 8 Comparison between overall runoff coefficient probability distribution and the probability distribution of runoff coefficients that give the match between rainfall and runoff return period.

#### References

- Chapman, T., & Maxwell, A. P. (1996). Baseflow separation - comparison of numerical methods with tracer experiments.  
 Viglione, A., Merz, R., & Blöschl, G. (2009). On the role of the runoff coefficient in the mapping of rainfall to flood return period. Hydrology and Earth System Sciences, 577-593. doi:10.5194/hess-13-577-2009  
 Merz, R., Blöschl, G., & Parajka, J. (2006). Spatio-temporal variability of event runoff coefficients. Journal of Hydrology, 331 (3), 591-604. https://doi.org/10.1016/j.jhydrol.2006.06.008

# References

- Berghuijs, W. R., Woods, R. A., Hutton, C. J., & Sivapalan, M. (2016). Dominant flood generating mechanisms across the united states. *Geophysical Research Letters*, *43*(9), 4382-4390. Retrieved from <https://agupubs.onlinelibrary.wiley.com/doi/abs/10.1002/2016GL068070> doi: <https://doi.org/10.1002/2016GL068070>
- Beurton, S., & Thielen, A. (2009, 02). Seasonality of floods in germany. *Hydrological Sciences Journal-journal Des Sciences Hydrologiques - HYDROLOG SCI J*, *54*, 62-76. doi: 10.1623/hysj.54.1.62
- Breinl, K., Lun, D., Müller-Thomy, H., & Blöschl, G. (2021). Understanding the relationship between rainfall and flood probabilities through combined intensity-duration-frequency analysis. *Journal of Hydrology*, *602*, 126759. Retrieved from <https://www.sciencedirect.com/science/article/pii/S002216942100809X> doi: <https://doi.org/10.1016/j.jhydrol.2021.126759>
- Chapman, T., & Maxwell, A. P. (1996). Baseflow separation - comparison of numerical methods with tracer experiments.
- Chow, V. T. (1964). Handbook of applied hydrology.
- Gaál, L., Szolgay, J., Kohnová, S., Parajka, J., Merz, R., Viglione, A., & Blöschl, G. (2012). Flood timescales: Understanding the interplay of climate and catchment processes through comparative hydrology. *Water Resources Research*, *48*(4). Retrieved from <https://agupubs.onlinelibrary.wiley.com/doi/abs/10.1029/2011WR011509> doi: <https://doi.org/10.1029/2011WR011509>
- Giani, G., Tarasova, L., Woods, R. A., & Rico-Ramirez, M. A. (2022). An objective time-series-analysis method for rainfall-runoff event identification. *Water Resources Research*, *58*(2), e2021WR031283. Retrieved from <https://agupubs.onlinelibrary.wiley.com/doi/abs/10.1029/2021WR031283> (e2021WR031283 2021WR031283) doi: <https://doi.org/10.1029/2021WR031283>
- Lun, D., Viglione, A., Bertola, M., Komma, J., Parajka, J., Valent, P., & Blöschl, G. (2021). Characteristics and process controls of statistical flood moments in europe – a data-based analysis. *Hydrology and Earth System Sci-*

## References

---

- ences, 25(10), 5535–5560. Retrieved from <https://hess.copernicus.org/articles/25/5535/2021/> doi: 10.5194/hess-25-5535-2021
- Merz, R., & Blöschl, G. (2009). A regional analysis of event runoff coefficients with respect to climate and catchment characteristics in Austria. *Water Resources Research*, 45(1). doi: <https://doi.org/10.1029/2008WR007163>
- Merz, R., Blöschl, G., & Parajka, J. (2006). Spatio-temporal variability of event runoff coefficients. *Journal of Hydrology*, 331(3), 591–604. doi: <https://doi.org/10.1016/j.jhydrol.2006.06.008>
- Parajka, J., Merz, R., & Blöschl, G. (2005). A comparison of regionalisation methods for catchment model parameters. *Hydrology and Earth System Sciences*, 9(3), 157–171. Retrieved from <https://hess.copernicus.org/articles/9/157/2005/> doi: 10.5194/hess-9-157-2005
- Sivapalan, M., Blöschl, G., Merz, R., & Gutknecht, D. (2005). Linking flood frequency to long-term water balance: Incorporating effects of seasonality. *Water Resources Research*, 41(6). Retrieved from <https://agupubs.onlinelibrary.wiley.com/doi/abs/10.1029/2004WR003439> doi: <https://doi.org/10.1029/2004WR003439>
- Tarasova, L., Basso, S., Zink, M., & Merz, R. (2018). Exploring controls on rainfall-runoff events: 1. time series-based event separation and temporal dynamics of event runoff response in Germany. *Water Resources Research*, 54(10), 7711–7732. Retrieved from <https://agupubs.onlinelibrary.wiley.com/doi/abs/10.1029/2018WR022587> doi: <https://doi.org/10.1029/2018WR022587>
- Viglione, A., & Blöschl, G. (2009a). On the role of storm duration in the mapping of rainfall to flood return periods. *Hydrology and Earth System Sciences*, 13(2), 205–216. Retrieved from <https://hess.copernicus.org/articles/13/205/2009/> doi: 10.5194/hess-13-205-2009
- Viglione, A., Merz, R., & Blöschl, G. (2009b). On the role of the runoff coefficient in the mapping of rainfall to flood return periods. *Hydrology and Earth System Sciences*, 13(5), 577–593. Retrieved from <https://hess.copernicus.org/articles/13/577/2009/> doi: 10.5194/hess-13-577-2009